Characterization of a Well-Type HPGe Detector Using Standards

A Major Qualifying Project Report
Submitted to the faculty of
WORCESTER POLYTECHNIC INSTITUTE
In partial fulfillment of the requirements for the
Degree of Bachelor of Science

Submitted to:
Stephen J. Kmiotek

By:
Jolina T. Alonzo

11 December 2022

Advised by:
Dr. Bruce D. Pierson (PNNL)

ABSTRACT

The characterization of the WELL3 detector, a well-type detector, at Pacific Northwest National Laboratory (PNNL) is an important and necessary capability for performing high-precision, low-intensity radio-isotope measurements. The characterization of the WELL3 detector provided the Advanced Radio-Emission Spectroscopy (ARES) team with another detector to analyze and obtain data for weak radioactive isotopes. A benchmarked calibrated and characterized model of the WELL3 detector was created using the CERN C++ particle simulation framework GEANT4[1] with a PNNL developed utility, the Geant4-Cascade Summing Correction tool[2]. This benchmark was constructed by conducting quantitative intercomparison of the modeled and measured detector response to a National Institute of Standards & Technology (NIST) traceable mixed gamma standard mix 7503 from Eckert & Zeigler and a medical isotope standard of Molybdenum-99 (Mo-99) from the National Physical Laboratory. The mixed gamma standard, NIST traceable measured detection efficiency, was used to optimize the model parameters before conducting an independent validation using the Mo-99 standard. A comparison of peak ratios was performed between the measured and simulated spectra of Mo-99 to analyze the accuracy of the decay cascade summing probabilities predicted by the model. From the counted Mo-99 sample the half-life ($T_{1/2}$) was obtained for each relevant gamma ray energy lines and compared against the Evaluated Nuclear Structure Data Files (ENSDF) available from the National Nuclear Data Center. The analysis of the true-coincidence summing (TCS) corrections of the Mo-99 response from the benchmarked model show large corrections were made to simulate the spectrum from Mo-99 on WELL3. The future work will encompass further optimization of the calibrated detector model on GEANT4 with G4CSC. The current characterization of the WELL3 detector shows promise for the counting of Tb-161, an important nuclide in medical physics. Overall, the characterization of the WELL3 detector at PNNL now provides the ARES team a new capability for the high-efficiency detection of weak samples.

---

[1] S. Agostinelli *et al.*, “Geant4—a simulation toolkit,” *Nuclear Instruments and Methods in Physics Research Section A: Accelerators, Spectrometers, Detectors and Associated Equipment*, vol. 506, no. 3, pp. 250–303, Jul. 2003, doi: 10.1016/S0168-9002(03)01368-8.

[2] B. Pierson, B. Archambault, A. Hagen, and C. Soren, “G4CSC.” Accessed: Nov. 30, 2022. [Online]. Available: https://gitlab.pnnl.gov/ares/g4csc

SUMMARY

Introduction

A well-type high purity germanium (HPGe) detector has the capability to place samples inside the detector. This distinct characteristic results in a high detection efficiency for the activity measurement of gamma ray emissions from the decay scheme of a radioactive sample. This detector is the most sensitive form of the HPGe detector since provides the maximum feasible sensitivity for weak samples of radioactive isotopes. The characterization of the WELL3 detector, a well-type detector, at Pacific Northwest National Laboratory (PNNL) is important to provide the capability of a well-type detector for sample analysis. Overall, the characterization of the WELL3 detector at PNNL provides the Advanced Radio-Emission Spectroscopy (ARES) team with another detector to analyze and obtain data for a wide range of radioactive isotopes.

Experimental Description

A calibration sample was obtained to start the process of the characterization of the WELL3 detector. The calibration sample was then counted on the WELL3 detector. A benchmarked calibrated and characterized model of the WELL3 detector was created using GEANT4[1, p. 4] software. The process was based on creating an optimized detector model using the instrument specifications sheet from the manufacturer and physical measurements taken in the laboratory. With the benchmarked model of the WELL3 detector, Molybdenum-99 (Mo-99) was simulated to produce a spectrum of the detector model response. A single-isotope nuclide gamma standard of Mo-99 was counted on the WELL3 detector over ~40 days to produce 26 resulting spectra. Over 10 half-life ($T_{1/2}$) occurred over the counting period. The $T_{1/2}$ was obtained for each relevant gamma ray energy line and compared against the National Nuclear Data Center's Evaluated Nuclear Structured Data File (ENSDF) value available. A comparison of relevant nuclear data was performed between the measured and simulated spectra of Mo-99. The peak area of the measured spectrum and bin counts of the simulated spectrum were compared as peak ratios to analyze the accuracy of the benchmarked detector model. An analysis of the true-coincidence summing (TCS) corrections was performed, based upon measuring geometry, detector dimensions and the decay scheme of the radioactive isotope.

Initial WELL3 Detector Model

Once the input script to the detector modeling software was complete with detector measurements and required nuclear data of the calibration isotopes, it was then modeled to produce a representation of the measured spectrum. Iterative comparisons between the overall detection efficiency of the measurement and simulated detector models were performed to find an optimized representation of the detection system. Model estimates derived from the manufacturer specification sheet, detailed in *Appendix B*, indicated the detector model was inadequate since the overall detection efficiency did not match between the simulated and the measured data. The calibration and characterization of the detector model was not complete, therefore multiple iterations with adjustments to detector dimensions were performed using GEANT4 with G4CSC.

Benchmarked WELL3 Detector Model

The creation of a benchmarked detector model required adjustments to the can gap, dead layer thickness and sample placement from educated predictions for the detector response. The process method described previously to produce the detector model response of the calibration sample was performed. A comparison between the overall detection efficiency of the measured and simulated detector model was performed. The analysis indicated the initial detector model under-estimated the inner dead-layer thickness and sample positioning. After making several adjustments the model was effectively benchmarked by demonstrating good agreement between the measured detector efficiency and simulation. The WELL3 detector was deemed effectively characterized through this comparison and was then used in the analysis of the Mo-99 radioactive isotope.

Mo-99 Comparison Analysis

A single-isotope gamma standard of Mo-99 was obtained from the National Physical Laboratory and counted on the WELL3 detector at PNNL. The sample was counted for approximately 40 days, where over 10 $T_{1/2}$ occurred during that period. The sample counting resulted in 26 spectra which were analyzed using the Mirion Genie2000 software. The measured spectrum of Mo-99 was also generated using the benchmarked detector model for comparison to the measured results. The peak area of the measured spectrum and bin counts of the simulated spectrum were compared as peak ratios to analyze the accuracy of the benchmarked detector model. The inter-comparison of the peak ratios showed adequate agreement. The predicted true-coincidence summing corrections for Mo-99 counting derived from the benchmarked model show large corrections were necessary to accurately quantify Mo-99 using a well-type HPGe detector as expected.

$T_{1/2}$ Analysis of Mo-99

An analysis of $T_{1/2}$ was performed for the mixed gamma sample of Mo-99 using the WELL3 detector at PNNL. The sample was counted for ~40 days, where over 10 $T_{1/2}$ occurred during that period. The sample counting resulted in 26 spectra which were analyzed using the Mirion Genie2000 software, with regions of interest from ~40keV to ~1200keV. The Genie200 software was used for peak analysis of all single and complex spectral features. After the peak fitting was complete, the $T_{1/2}$ at each significant gamma ray energy line was calculated. Overall, the disadvantages of peak summing in the WELL3 detector make it less than ideal for the measurement of Mo-99, nevertheless, the $T_{1/2}$ isotope was accurately measured and agreed well with the known published value while also serving as an excellent test reference for the consistency performance of the WELL3 detector at PNNL.

Conclusion

The characterization of the WELL3 detector was performed with a mixed gamma standard and a single-isotope standard of Mo-99. To calibrate the WELL3 detector, a benchmarked model was created using GEANT4 and G4CSC. Future work will encompass further optimization of the calibrated detector model on GEANT4 with G4CSC. The current characterization of the WELL3 detector shows promise for the counting of Tb-161 an important nuclide for emerging medical physics studies. Overall, the characterization of the WELL3 detector at PNNL now provides the ARES team a new capability for the high efficiency counting of weak radioisotopes.

ACKNOWLEDGEMENTS

I would like to thank PNNL for the opportunity to use their laboratories and technologies and work alongside other researchers. A special thanks to Dr. Bruce Pierson for his support, guidance, and mentorship in performing radiation detection and measurement studies, as well as Ms. April Augustine for an enriching program. I would also like to acknowledge and thank DTRA for sponsoring my project and giving me this opportunity. Finally, I would like to extend my gratitude to WPI for this unique opportunity and to Professor Stephen Kmiotek for his unwavering support and all the subsequent work he has undertaken to make this project site a success.

NOMENCLATURE

ARES – Advanced Radio-Emission Spectroscopy

CERN C++ - Analyzing petabytes of data, scientifically for high energy physics

ENSDF – Evaluated Nuclear Structured Data File

GEANT4 with G4CSC - Toolkit for the simulation of the passage of particles through matter

HPGe – High Purity Germanium

keV – kiloelectronvolts

Mo-99 – Molybdenum-99

NIST - National Institute of Standards and Technology

PNNL – Pacific Northwest National Laboratory

ROI – Region of Interest

sec – seconds

TCS – True Coincidence Summing

TABLE OF CONTENTS

TABLE OF FIGURES

TABLE OF TABLES

1.0 INTRODUCTION

A high purity germanium (HPGe) detector provides a researcher with reliable information to accurately identify radioactive isotopes based on passive gamma ray emissions from the decay scheme. A HPGe detector requires the sample to be placed on top, while a well-type HPGe detector has the capability to place samples inside the detector. This distinct characteristic results in high detection efficiency for the activity measurement of gamma ray emissions from the decay scheme of a radioactive isotope sample. A well-type detector can be considered one of the more sensitive forms of an HPGe detector since it is capable of achieving very high counting efficiency.

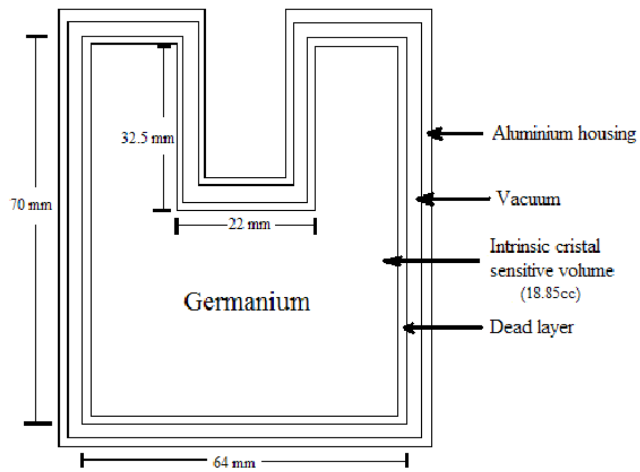

Figure 1. General model of a HPGe Well-type detector[3]

The characterization of the WELL3 detector, a well-type detector, at PNNL is important to provide the capability and usability of a well-type detector for samples. The Advanced Radio-Emission Spectroscopy (ARES) team at Pacific Northwest National Laboratory (PNNL) wants to maintain a broad range of detectors to measure relevant radioactive isotopes. The ability to detect low- and high-activity samples is needed by the Advanced Radio-Emission Spectroscopy (ARES) team to support research & development at PNNL. However, a disadvantage to the WELL3 detector is that it is most difficult to use for quantitative analysis due to complex detector physics effects induced by nested nuclear decay chains. This type of analysis is a technique that uses

[3] Carvalho Conti, C. (n.d.). *Schematic figure of HPGE well detector cross section*. Research Gate. Retrieved July 18, 2022, from https://researchgate.net/figure/Schematic-figure-of-HPGe-well-detector-cross-section_fig1_265109579

mathematical and statistical modeling, measurement, and research to understand the behavior of the samples. Overall, the characterization of the WELL3 detector at PNNL provides the ARES team with another detector to analyze and obtain data for weak samples.

2.0 EXPERIMENTAL DESCRIPTION

A calibration sample was obtained to start the characterization process of the WELL3 detector. A National Institute of Standards and Technology (NIST) traceable standard was obtained. The ARES team created a secondary standard derived from the primary standard mixture received from the Eckert & Zeigler. Production of internal secondary standards at PNNL is facilitated by the Analytical Support Operations service center which maintains a HASQARD compliant quality assurance program. The calibration sample was then counted on the WELL3 detector.

A benchmarked calibrated and characterized model of the WELL3 detector was created using GEANT4 modeling software. The process was based on creating an optimized detector model starting from the detector vendor specification sheet from the manufacturer, detailed in *Appendix B*, and physical measurements taken in the lab. Once all required measurements were obtained, it was applied to the model. The detector and calibration source model were created to predict the spectral response of the instrument for comparison to measurements. The detector spectral response was predicted for each isotope in the standard and combined using the data analysis framework CERN C++. The combined simulated spectrum and efficiency were used to evaluate the accuracy of the model.

A single nuclide gamma standard of Molybdenum-99 (Mo-99) was counted on the WELL3 detector over approximately 40 days to produce 26 spectra. Over 10 half-lives ($T_{1/2}$) occurred during the counting period. Each spectrum was analyzed using Mirion's Genie2000 software for peak fitting of the relevant gamma ray energy lines produced by the sample. The $T_{1/2}$ was obtained for each relevant gamma ray energy lines and compared against the Evaluated Nuclear Structured Data File (ENSDF) value.

A comparison of relevant nuclear data was performed between the measured and simulated spectra of Mo-99. The peak area of the measured spectrum and bin counts of the simulated spectrum were compared as peak ratios to analyze the accuracy of the benchmarked detector model. An analysis of the true-coincidence summing (TCS) corrections was also performed based upon measuring geometry, detector dimensions, and the decay scheme of the radioactive isotope. TCS occurs when two or more photons are emitted from the decay scheme from the same decay of the radioactive isotope and subsequently detected simultaneously within the resolving time of the detector. This phenomenon occurs prolifically within well-type HPGe detectors and required to correct measurement data from such instruments.

3.0 INITIAL WELL3 DETECTOR MODEL

3.1 GEANT4 Modeling with G4CSC Response

The data required for the GEANT4 script input included the detector type, detector name, position in space (x, y, and z coordinates), rotation in space (ϕ and θ), hole depth, hole diameter, inner dead layer, outer dead layer, detector diameter, detector length, detector bevel radius, detector can gap, can thickness, can diameter, can material, and manufacturer. The script required the measurements and characteristics of the sample as well – sample name, position in space, rotation in space, source diameter, container diameter, container base thickness, source height, source material, and container material. Once the input script was complete, it was then run with the GEANT4 software to produce the initial detector model.

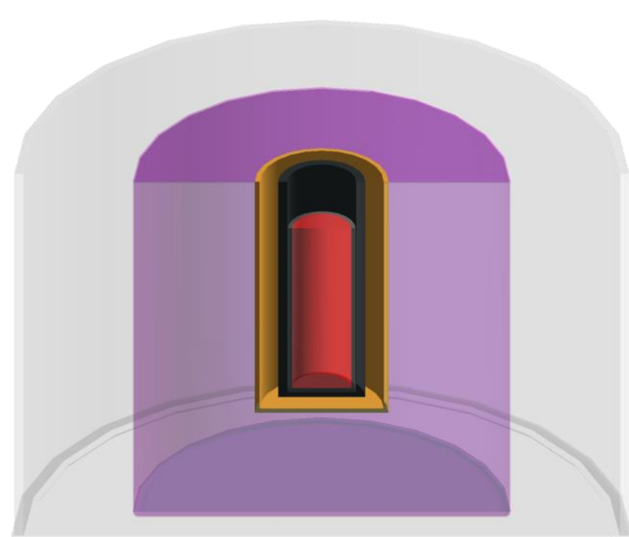

Figure 2. Initial WELL3 detector model with GEANT4

An input script that contained the relevant nuclear data of the 12 radioactive isotopes in the calibration sample was used to estimate the detector response. The contents of this standard included Co-60, Pb-210, Am-241, Te-123m, Cd-109, Co57, Sn-113, Sr-85, Mn-54, Y-88, Zn-65, and Cs-137. After the script was run through the appropriate software, individual spectra of each calibration isotope were produced. For each spectrum, the gamma ray energy line with the largest bin count was extracted and scaled appropriately into a resulting spectrum of the calibration sample utilizing CERN C++. The scaling was based upon the ratio of the bin count in the simulated spectrum to the peak area in the measured calibration sample spectrum. The process was done for each of the 12 radioactive isotopes of the calibration sample.

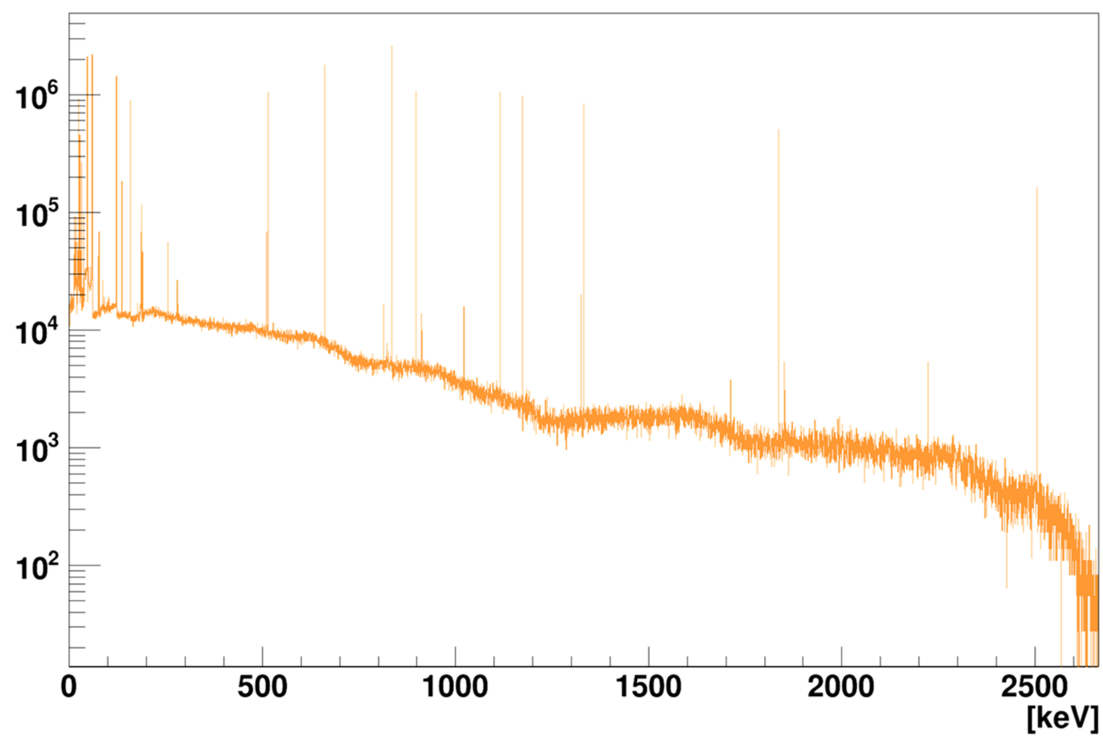

Figure 3. Initial simulated gamma-ray energy line spectrum of calibration sample from CERN C++

3.2 Comparison of Measured vs. Simulated Response

A comparison between the overall detection efficiency of the measured model and simulated detector model was performed. The appropriate files which provided the overall detection efficiency at the relevant gamma ray energy lines were obtained for analysis. A scatter plot was created in Excel® to show the overlapping of the measured and simulated response.

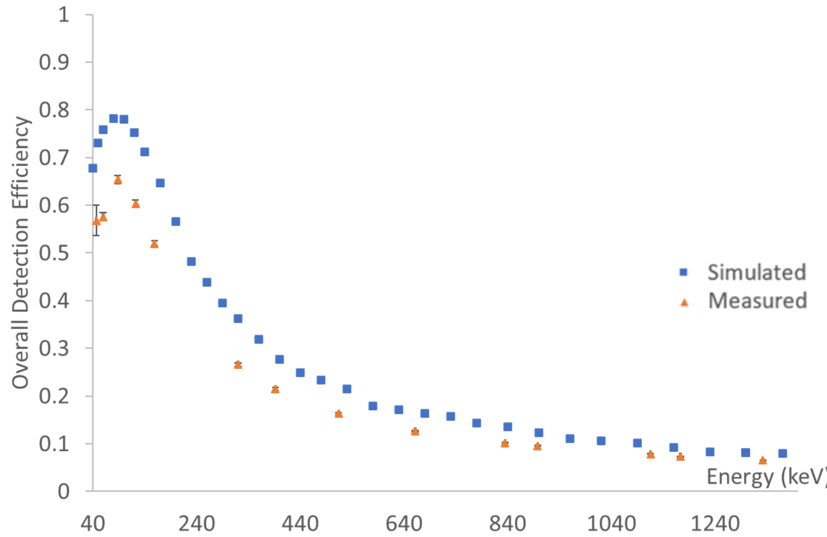

Figure 4. Overall Detection Efficiency vs. Energy (keV)

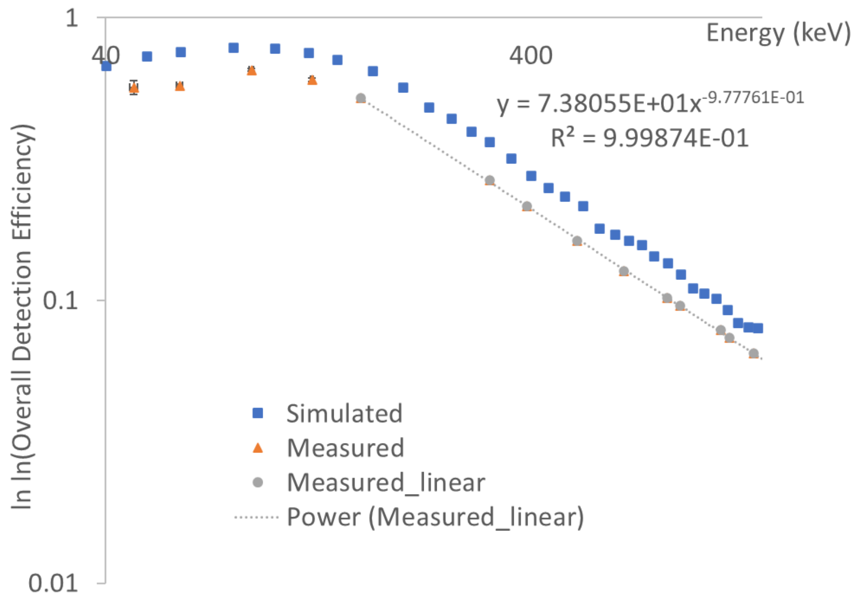

Figure 5. ln ln(Overall Detection Efficiency) vs. Energy (keV)

The scatter plots indicate the detector model was inadequate since the overall detection efficiency did not match between the simulated and the measured data. The two data sets show minimal overlapping further verifying the previous statement. The calibration and characterization of the detector model required multiple iterations with adjustments to multiple detector dimensions to obtain good agreement between the modeled and measured efficiency.

4.0 BENCHMARKED WELL3 DETECTOR MODEL

4.1 GEANT4 Modeling with G4CSC Response

The creation of a benchmarked detector model required adjustments to the can gap, dead layer thickness and sample placement using expert judgement and additional measurements. A thicker dead layer and an increased sample placement height was the result to create the benchmarked detector model. The dead layer thickness and can gap were unknown since they were measurements not initially recorded when the WELL3 detector was made. The sample placement needed educated predictions since the sample is placed in a plastic bag when inserted into the detector hole. The plastic bag creates uncertainty to where the sample is placed inside the hole. The benchmarked dimensions of the detector model were inputted into the script and run using GEANT4 with G4CSC to produce the calibration sample response.

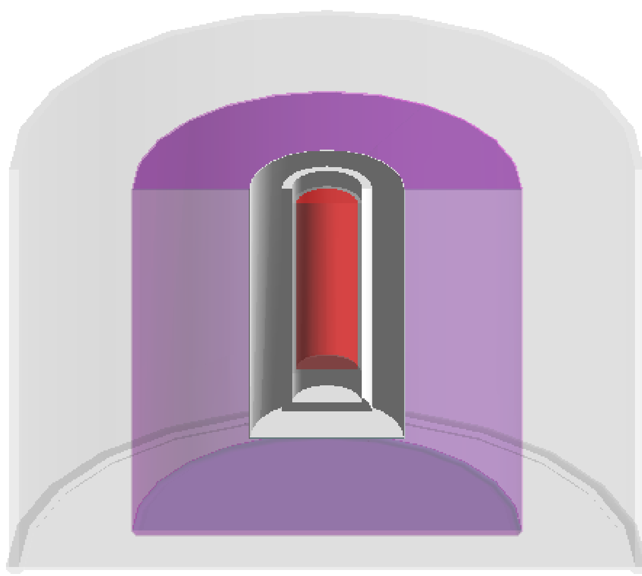

Figure 6. Benchmarked WELL3 detector modeled with GEANT4

The process method described above in *Section 3.1* to create the resulting spectrum of the calibration sample from the benchmarked model utilizing CERN C++ was repeated.

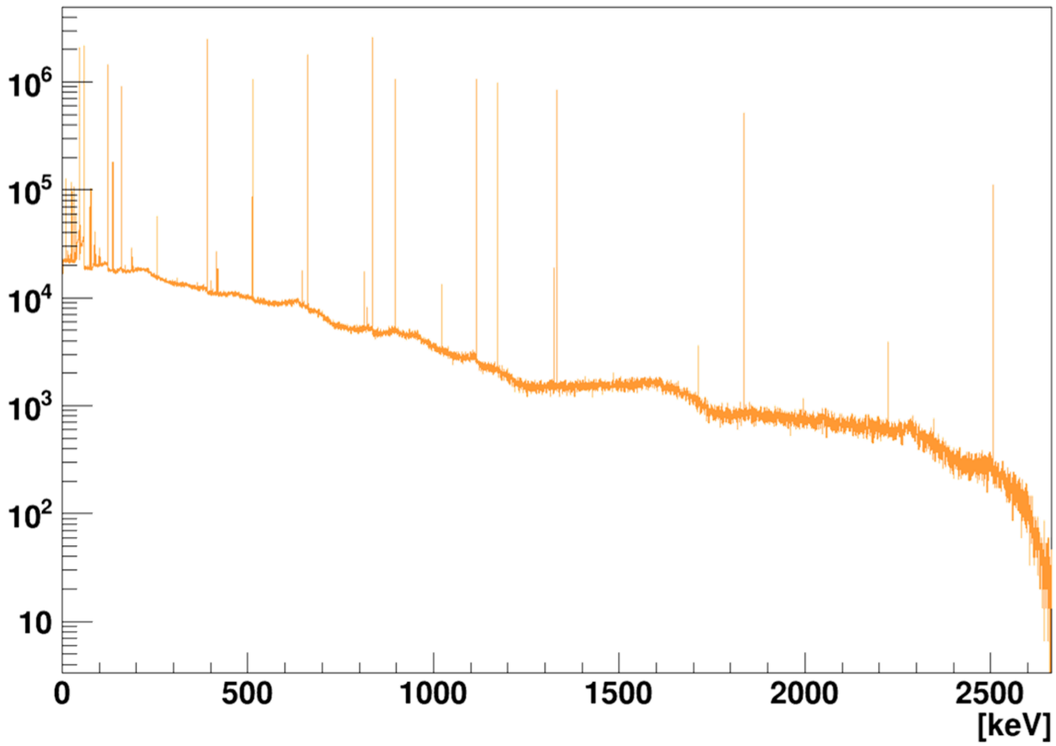

Figure 7. Benchmarked simulated gamma-ray energy line spectrum of calibration sample from CERN C++

4.2 Comparison of Measured vs. Simulated Response

A comparison between the overall detection efficiency of the measured model and simulated detector model was performed. The appropriate files which provided the overall detection efficiency at the relevant gamma ray energy lines were obtained for analysis. A scatter plot was created in Excel© to show the overlapping of the measured and simulated response.

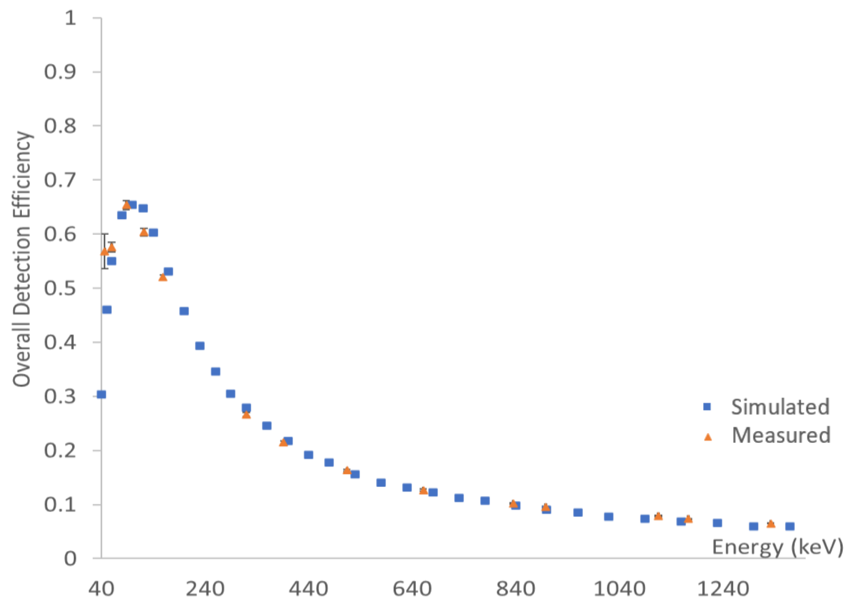

Figure 8. Overall Detection Efficiency vs. Energy (keV)

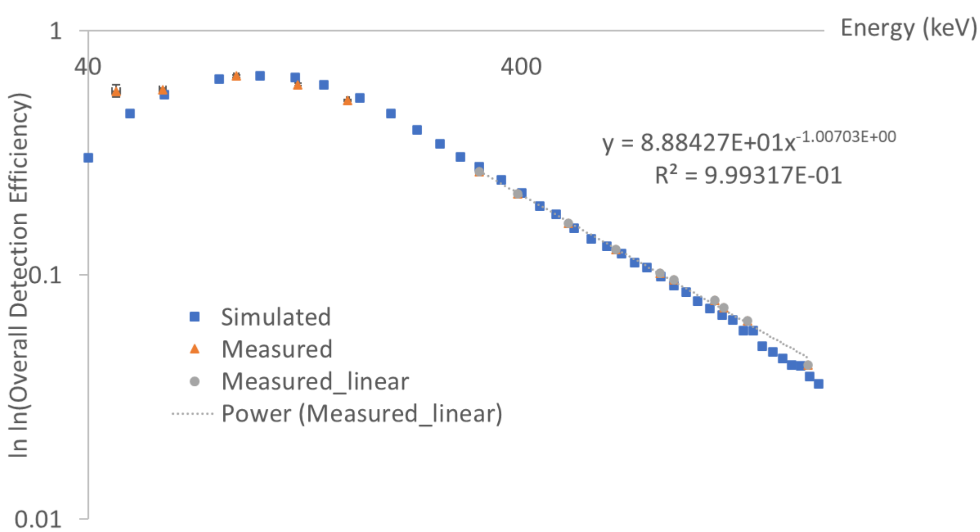

Figure 9. ln ln(Overall Detection Efficiency) vs. Energy (keV)

The scatter plots indicate the detector model was effectively benchmarked based on the good comparison between the overall detector efficiency of the measured and simulated data. The WELL3 detector was deemed effectively characterized through this comparison and validation was performed using as separate set of metrics and a different source.

5.0 MO-99 COMPARISON ANALYSIS

5.1 Mo-99 Counted on WELL3

A single nuclide gamma standard of Mo-99 was obtained to be counted on the WELL3 detector at PNNL. The sample was counted for approximately 40 days, where over 10 $T_{1/2}$ occurred during that period. The sample counting resulted in 26 spectra which were analyzed using the Mirion Genie2000 software, with regions of interest (ROI) spanning ~40keV to ~1200keV.

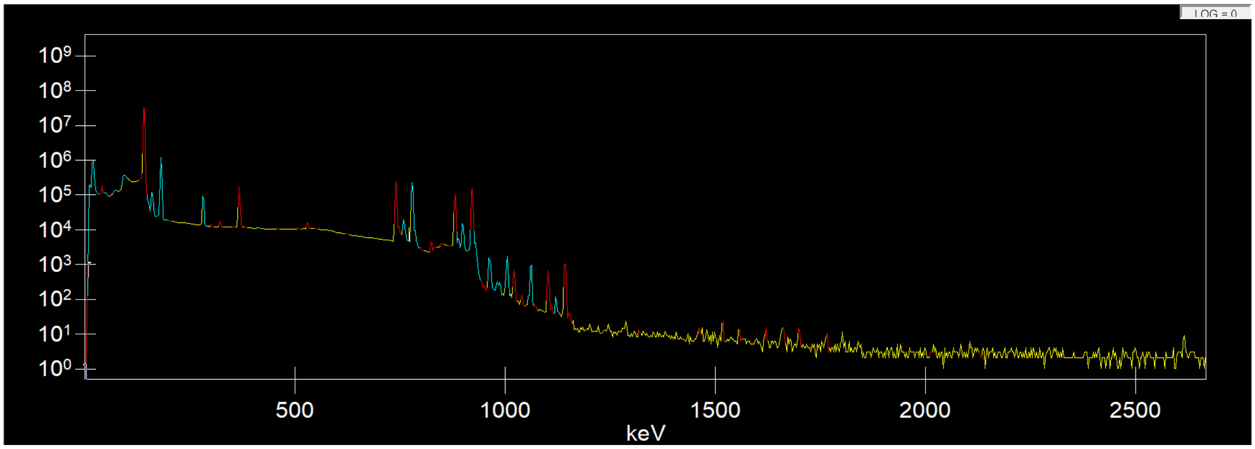

Figure 10. A spectrum the first count of Mo-99 from WELL3, displayed by the Mirion Genie2000

A simulated response of Mo-99 on the benchmarked detector was obtained using the input script described in *Section 4.1*, including the required nuclear data of Mo-99. A simulated response with TCS corrections was produced using GEANT4 with G4CSC.

5.2 Mo-99 Simulated Response on Benchmarked Model

A simulated response of Mo-99 on the benchmarked detector was obtained using the input script described in *Section 4.1*, including the required nuclear data of Mo-99. A simulated response with TCS corrections was produced using GEANT4 with G4CSC.

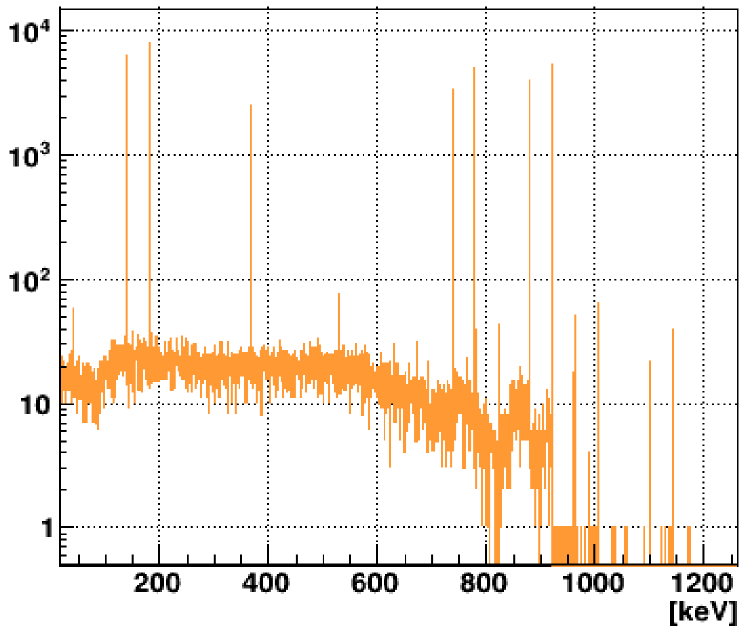

Figure 11. A simulated spectrum of Mo-99 produced with the benchmarked model, displayed by CERN C++

5.3 Comparison of Mo-99 Measured vs. Simulated Response

The comparison required obtaining data from measured counts of Mo-99 on WELL3 and the simulated response of Mo-99 on the benchmarked model. For an in-depth analysis, measured counts of Mo-99 had to meet the following requirements – contained all the significant gamma ray energy lines and was chosen at different times of counting. The spectrum of counts 1, 2, 3 and 12 were compared against the simulated Mo-99 response, using a peak ratio comparison.

The peak area of the measured spectrum and bin counts of the simulated spectrum were compared as peak ratios to analyze the accuracy of the benchmarked detector model. To compare the peak ratios, the peak areas/bin counts of interest corresponded to the following gamma ray energy lines: 40.52, 181.1, 366.5, 528.6, 739.5, 778.1, 880.0, and 920.6 keV. The 739.5 keV gamma ray energy line was used for reference during the calculation of the peak ratios for each spectrum of interest, referenced in the equation below.

$$peak\ ratio = \frac{count_n}{count_{739.5keV}} \quad [1]$$

Table 1. Comparison of measured and simulated peak ratio to the main gamma ray energy line at 739.5 keV

	Gamma Ray Energy Line (keV)	*40.52*	*181.1*	*366.5*	*528.6*	*739.5*	*778.1*	*880.0*	*920.6*	*1004.0*
1	-	0.2450	0.4105	0.5723	0.01928	1*	1.036	0.4760	0.7280	0.00796
2	-	0.2280	0.3950	0.5750	0.01870	1*	0.9770	0.4400	0.6720	0.00793
3	-	0.2250	0.3840	0.5570	0.01940	1*	0.9810	0.4500	0.6990	0.00737
12	-	0.2240	0.3830	0.5640	0.02020	1	0.9940	0.4570	0.6990	0.00710
Sim.	-	0.1370	0.3949	0.5941	0.01803	1*	1.034	0.6341	0.8604	0.00830

An analysis of the calculated peak ratios showed adequate agreement for the most intense gamma-ray emissions, but some discrepancy was observed for the more uncertain gamma-lines (880, 920.6, and 1004 keV). A clear discrepancy at 40.52 keV is likely the by-product of errors in the model dead-layer but could possibly point to issues in the decay feeding of this gamma-line.

The final analysis between the simulated response of Mo-99 was based on the TSC corrections obtained from the data file produced from GEANT4 with G4CSC.

Table 2. Measured activity from Mo-99 detector model response with TCS corrections

Gamma Ray Energy Line (keV)	***TCS Corrections***
40.47	0.1137
140.4	0.3664
158.8	0.1765
181.1	0.3669
366.4	0.9862
528.6	1.074
739.6	0.2339
778.0	1.002

The analysis of the TCS corrections of the Mo-99 response from the benchmarked model show large corrections were made to simulate the spectrum from Mo-99 on WELL3. If the TCS corrections were small, the numbers would be closer to 1, indicating less corrections were done. However, most gamma ray energy lines show a large TCS correction factor. For low energy samples in combination with another photon, the TCS corrections are more pronounced for a detector that has a high efficiency for low energy photons, like a well-type detector. If TCS corrections were not corrected for, the activity of the sample could be over- or underestimated.

6.0 $T_{1/2}$ Analysis of Mo-99

An analysis of $T_{1/2}$ was performed for the mixed gamma sample of Mo-99 using the WELL3 detector at PNNL. The sample was counted for approximately 40 days, where over 10 $T_{1/2}$ occurred during that period. Peak fitting required careful analysis of the spectral features in the Mo-99 spectra. The insignificant peaks that did not match criteria were had to be removed as well. To further improve peak fitting, some ROIs of the peaks were adjusted to the correct region for the peak. The technique was used to clean up the inconsistency of the peaks in the spectrum due to the complexity and overlap in the spectrum from TCS effects. Another factor that contributed to complex peaks was peak summing, a phenomenon that occurs when only one detector is used; the detector will sum together two peaks to create random "sum peaks."

After the peak fitting was complete, the $T_{1/2}$ at each significant gamma ray energy line was calculated. The following data was needed from each count to perform the $T_{1/2}$ calculation: energy (keV), net peak area, realtime (sec), livetime (sec), and the time difference based on the initial count. The data needed to be analyzed for each count to ensure the proper net peak area was chosen for the corresponding gamma line.

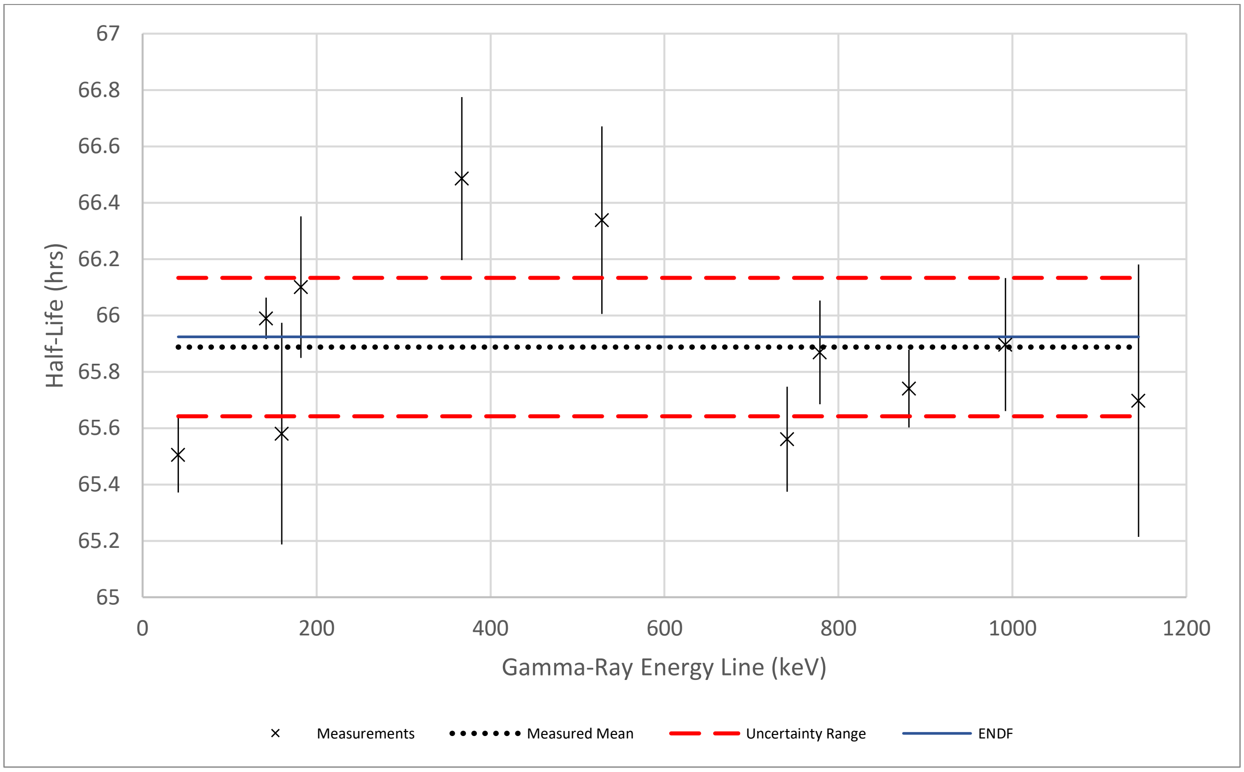

Figure 12. T1/2 comparisons with the corresponding gamma ray energy lines

The ENDF value, 65.924 hours, is shown on the graph which compares well to the $T_{1/2}$ calculated at 142 keV. The $T_{1/2}$ obtained at 142 keV, 65.990 +/- 0.0733 hours, shows comparability to the ENDF value, verified by the smallest standard deviation, which is within 1σ of the ENDF value. The average $T_{1/2}$ calculated for the significant gamma ray energy lines compares relatively well to the ENDF value at 65.888 +/- 0.246 hours. Overall, given the disadvantages of peak summing in the WELL3 detector it is not ideally suited for measuring the Mo-99 but the performance of the instrument over this protracted count period served as a test of the consistent reliable operation of this instrument.

7.0 CONCLUSION

The characterization of the WELL3 detector was performed with a mixed gamma standard of Mo-99. To calibrate the WELL3 detector, a benchmarked model was created using GEANT4 with G4CSC. The benchmarked model required adjustments of the can gap, increased dead layer thickness, and higher sample placement through educated predictions of the detector model response. A relevant piece of nuclear data for Mo-99 obtained by WELL3 was the $T_{1/2}$ analysis. It was an adequate detector for the analysis however the variation can be attributed to the counting statistics and the peak fitting uncertainty.

The future work will encompass further optimization of the calibrated detector model on GEANT4 with G4CSC. This will require more iterations of educated predictions of the sample placement and crystal size. The current characterization of the WELL3 detector shows promise for the counting of Tb-161 which is a relevant nuclide to nuclear forensics and medical physics. The nuclide is also an important fission product for estimating the total fissions in experimental samples. Overall, the characterization of the WELL3 detector at PNNL now provides the ARES team a new capability for the high efficiency counting of weak samples, a capability not initially available.

APPENDICIES

Appendix A – Counted Samples

Mo-99 Sample

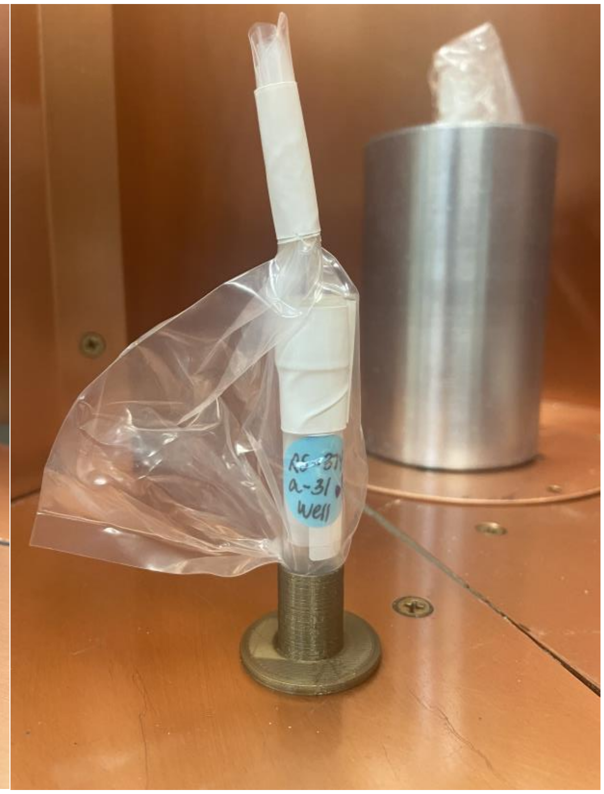

Calibration Sample

Appendix B – Canberra Specification Sheet

Replaces Ortec Det WELL3
New Det 3

CANBERRA

Rev. 6/15/99

DETECTOR SPECIFICATION AND PERFORMANCE DATA

Specifications

DETECTOR MODEL GCW3523S SERIAL NUMBER 11051527
CRYOSTAT MODEL 7500SL/RDC/ULB PREAMPLIFIER MODEL 2002CSL

The purchase specifications, and therefore the warranted performance, of this detector are as follows:
(Electric cooling may degrade performance by as much as 10%.)

Active Volume ______ cc Relative Efficiency 35 %
Resolution ≤2.3 keV (FWHM) at 1.33 MeV
______ keV (FWTM) at 1.33 MeV
≤1.4 keV (FWHM) at 122KeV
______ keV (FWTM) at ______

Peak/Compton ______ :1 Cryostat well diameter 14.5 mm Cryostat well depth 40 mm

Cryostat description (if special) 3.25" Ø End Cap, 4" long RDC and Vertical Slimline dipstick cryostat and Ultra low Background cryostat hardware.

Physical Characteristics

Geometry Closed-end coaxial well
✓Diameter 61.5 mm
✓Length 63 mm
Distance from window 10 mm

Active Volume ______ cc
✓Well Depth 40.386 mm 1.590"
✓Well Diameter 14.1478 mm .557"

Electrical Characteristics

Depletion voltage (+)2600 V dc
Recommended bias voltage (+)3000 V dc
Test point voltage at recommended bias (-)0.81 V dc (RC preamp only)
Reset interval at recommended bias —— sec. (Reset preamp only)
Capacitance at recommended bias ~43 pF

Resolution and Efficiency

With amp time constant of 6 microseconds

Isotope	^{57}Co	^{60}Co			
Energy (keV)	122	1332			
FWHM (keV)	1.25	2.00			
FWTM (keV)	2.27	3.69			
Peak/Compton		50.9:1			
Rel. Efficiency %		35.3			

Cool Down Time 8 hours. Cryostat Liquid Nitrogen Consumption Rate <1.8 Liters per Day.

Tested by: Stephen Bishop Date: 11/23/05

Approved by: Wesley Moss Date: 11/23/05

800 Research Parkway, Meriden, CT USA 06450 • Tel. 203-238-2351/Fax. 203-639-2420

Appendix C – WELL3 Detector

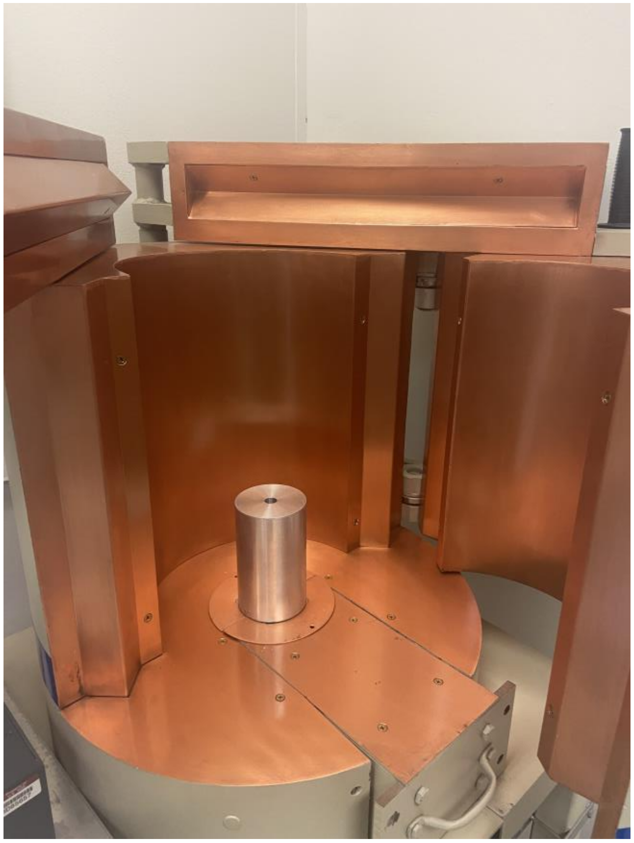

WELL detector

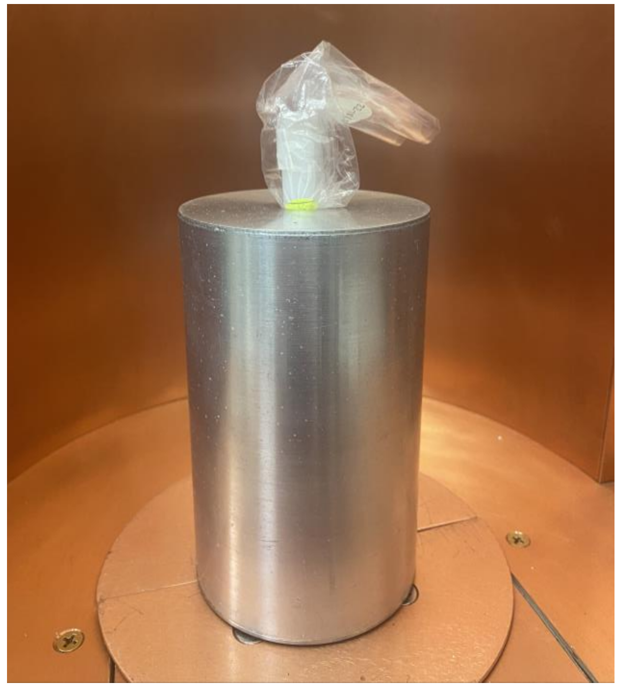

Standard in WELL detector

Appendix D – GEANT4 with G4CSC Script File

user.mac
~/Applications/g4csc-build

```
# ---------------------------------------------------------------------------
# **************************** SOURCE SELECTION ******************************
# ---------------------------------------------------------------------------
# DL=deadlayer
# ---------------------------------------------------------------------------
/vis/multithreading/actionOnEventQueueFull discard




#____________________________________________________________________________________________________________________________________
#/g4csc/src/cylindricalshape <name>          <x> <y> <z> <phi> <theta> <source_dia> <container_dia> <container_base_thickness> <source_height> <source_material>
<container_material>
 /g4csc/src/cylindricalshape  p0psv2mlw      0   0  28   0      0      9.627          11.                 0.762                  30.          G4_WATER      G4_POLYETHYLENE

# ---------------------------------------------------------------------------
# *************************** DETECTOR SELECTION ******************************
# ---------------------------------------------------------------------------
# DL=deadlayer D,K, is PGT (bevel both sides)
# ---------------------------------------------------------------------------
#####/g4csc/det/detectorshape <type> <name> <x> <y> <z> <phi> <theta> <hole depth> <hole dia> <inner DL> <outer DL> <detector dia> <detector length> <detector bevel radius>
<detector can gap> <can thickness> <can dia> <can material>   <manuf.>
 /g4csc/det/detectorshape      Well  WELL3   0   0   0   180      0         40.37       14.15     0.0003      0.7          61.5           63.
1.5                        2.            1.0         100           G4_Al       canberra

# ---------------------------------------------------------------------------
# *************************** ISOTOPE SELECTION ******************************
# *************************** PARTICLE HISTORIES *****************************
# ---------------------------------------------------------------------------
# CERN root histogram definitions used for output of spectrum predictions
# ---------------------------------------------------------------------------
/gun/particle ion

##Co-60
 /g4csc/gun/target co60 1 86400. 27 60 0. 1
#/run/beamOn 1000000

##Pb-210
 /g4csc/gun/target pb210 1 86400. 82 210 0. 1
/run/beamOn 1000000

##Am-241
 /g4csc/gun/target am241 1 86400. 95 241 0. 1
/run/beamOn 1000000

##Te-123m
 /g4csc/gun/target te123m 1 86400. 52 123 247.5 1
/run/beamOn 1000000

##Cd-109m
 /g4csc/gun/target cd109 1 86400. 48 109 462.7 1
/run/beamOn 1000000

##Co-57
 /g4csc/gun/target co57 1 86400. 27 57 0. 1
/run/beamOn 1000000

##In-113m
 /g4csc/gun/target sn113 1 86400. 49 113 391.7 1
/run/beamOn 1000000
```

```

##Sn-113
 /g4csc/gun/target sn113 1 86400. 50 113 0. 1
/run/beamOn 1000000

##Sr-85
 /g4csc/gun/target sr85 1 86400. 38 85 0. 1
/run/beamOn 1000000

##Mn-54
 /g4csc/gun/target mn54 1 86400. 25 54 0. 1
/run/beamOn 1000000

##Y-88
 /g4csc/gun/target y88 1 86400. 39 88 0. 1
/run/beamOn 1000000

##Zn-65
 /g4csc/gun/target zn65 1 86400. 30 65 0. 1
/run/beamOn 1000000

##Ba-137m
 /g4csc/gun/target ba137m 1 86400. 56 137 661.7 1
/run/beamOn 1000000

# ----------------------------------------------------------------------------
# ******************************** COLORING **********************************
# ----------------------------------------------------------------------------
# visualization commands used to setup the coloring.
# ----------------------------------------------------------------------------
 # Set visibility of logical volumes
 /vis/drawVolume
 /vis/geometry/set/visibility World  0 false
 /vis/geometry/set/visibility active_Ge_logical 1 true
 /vis/geometry/set/visibility cu_coldfinger_logical   1 true
 /vis/geometry/set/visibility inner_deadlayer_logical   1 true
 /vis/geometry/set/visibility outer_deadlayer_logical   1 true
 /vis/geometry/set/visibility Ge_can_logical   1 true
 /vis/geometry/set/visibility lead_annulus_logical  1 true
 /vis/geometry/set/visibility G4_Fe_inner_cover_1_logical 1 true
 /vis/geometry/set/visibility G4_Cu_inner_cover_2_logical 1 true
 /vis/geometry/set/visibility sample_logical   1 true
 /vis/geometry/set/visibility sample_holder_logical  1 true

 # Set color of logical volumes: surface view
 /vis/viewer/set/style surface
 /vis/geometry/set/colour World      0 0.95 0.95 0.95 1
 /vis/geometry/set/colour active_Ge_logical   1 0.42 0.92 0.99 0.2
 /vis/geometry/set/colour cu_coldfinger_logical  1 0.99 0.27 0.00 1
 /vis/geometry/set/colour inner_deadlayer_logical   1 0.50 1.00 0.00 1
 /vis/geometry/set/colour outer_deadlayer_logical   1 0.99 0.00 0.99 0.2
 /vis/geometry/set/colour Ge_can_logical      1 0.51 0.51 0.51 0.1
 /vis/geometry/set/colour lead_annulus_logical   1 0.71 0.71 0.71 0.05
 /vis/geometry/set/colour G4_Fe_inner_cover_1_logical  1 0.51 0.51 0.51 1
 /vis/geometry/set/colour G4_Fe_inner_cover_2_logical  1 0.51 0.51 0.51 1
 /vis/geometry/set/colour G4_Cu_inner_cover_2_logical  1 0.99 0.27 0.00 1
 /vis/geometry/set/colour sample_logical      1 1.00 0.00 0.00 0.9
 /vis/geometry/set/colour holder_logical      1 1.00 1.00 1.00 0.2
 /vis/geometry/set/colour window_logical      1 1.00 1.00 0.00 0.1
```

```

 # Set color of logical volumes: wireframe w/ cut plane view
 #/vis/viewer/set/style wireframe
 #/vis/geometry/set/colour World   0 0.95 0.95 0.95 1
 #/vis/geometry/set/colour active_Ge_logical   1 0.42 0.92 0.99 1
 #/vis/geometry/set/colour cu_coldfinger_logical  1 0.99 0.27 0.00 1
 #/vis/geometry/set/colour inner_deadlayer_logical  1 0.50 1.00 0.00 1
 #/vis/geometry/set/colour outer_deadlayer_logical  1 0.99 0.00 0.99 1
 #/vis/geometry/set/colour Ge_can_logical 1 0.51 0.51 0.51 1
 #/vis/geometry/set/colour lead_annulus_logical   1 0.71 0.71 0.71 1
 #/vis/geometry/set/colour G4_Fe_inner_cover_1_logical  1 0.51 0.51 0.51 1
 #/vis/geometry/set/colour G4_Cu_inner_cover_2_logical  1 0.99 0.27 0.00 1
 #/vis/geometry/set/colour sample_logical 1 1.00 0.00 0.00 1
 #/vis/geometry/set/colour sample_holder_logical   1 1.00 1.00 1.00 1
 /vis/enable
 /vis/viewer/refresh
```

Appendix E - $T_{1/2}$ Raw Data Calculations

Note – All rows with cells highlighted in RED are omitted from calculations

	A	B	C	D	E	F	G	H	I	J	K	L	M	N	O	P	Q
1				`	Energy (keV) select	41											
2	Count	Count Start Date/Time	Time Diff. (days)	Realtime (sec)	Livetime (sec)	Net Peak Area	Net Count-rate (1/sec)	BAD		Log-Linear Fit							
3	1	5/25/2022 19:25	0	72870.9	62850.9	796700	12.67603169			2.539712942			0	2.539713		-2.5396E-01	2.5298E+00
4	2	5/26/2022 15:53	0.852928241	72838.1	64800	647500	9.992283951			2.30181319			0.852928	2.301813		5.2059E-04	6.6737E-03
5	3	5/27/2022 12:34	1.715266204	71216.6	64800	527900	8.146604938			2.097601268			1.715266	2.097601		9.9996E-01	1.4519E-02
6	4	5/28/2022 15:54	2.853668981	91600.8	85480.5	506300		5.922988					4.963646	1.280108		2.3797E+05	1.0000E+01
7	5	5/29/2022 17:21	3.914236111	90627	85939.3	400100		4.655612					5.918623	1.012022			
8	6	5/30/2022 18:32	4.963645833	82500.2	79148.7	284700	3.597026862			1.280107633			6.971887	0.750498		Half-life (hrs)	65.5056
9	7	5/31/2022 17:27	5.918622685	89247.6	86400	237700	2.751157407			1.012021699			8.615266	0.333492		`+/-	0.1340
10	8	6/1/2022 18:44	6.971886574	88584	86400	183000	2.118055556			0.750498477			12.86723	-0.73885			
11	9	6/3/2022 10:10	8.615266204	87840.1	86400	120600	1.395833333			0.333491608			13.91772	-0.98032			
12	10	6/4/2022 14:49	9.8084375	87463	86400	93500							14.9169	-1.2472			
13	11	6/7/2022 16:13	12.8672338	86930.5	86400	41270	0.477662037			-0.738851832			22.91881	-3.31476			
14	12	6/8/2022 17:26	13.91771991	62379.4	62075.3	23290	0.375189488			-0.98032408			26.05416	-4.07782			
15	13	6/9/2022 17:25	14.91689815	65471.1	65226	18740	0.287308742			-1.247197886							
16	14	6/10/2022	15.84828704	86639.7	86400	1464		0.016944									
17	15	6/11/2022 16:59	16.89908565	86590.7	86400												
18	16	6/13/2022 11:12	18.65796296	14087.3	14060.9	5663		0.402748									
19	17	6/14/2022 16:20	19.8721412	86518.9	86400												
20	18	6/15/2022 16:59	20.89899306	86499.8	86400												
21	19	6/17/2022 17:28	22.91880787	86469.1	86400	3140	0.036342593			-3.314764876							
22	20	6/20/2022 20:42	26.05415509	86451.1	86400	1464	0.016944444			-4.07781526							
23	21	6/22/2022 15:06	27.82043981	86447.2	86400												
24	22	6/24/2022 17:06	29.90413194	86440.8	86400												
25	23	6/28/2022 16:20	33.87206019	85129.2	85093.9						0	140.4276	4.944692				
26	24	6/29/2022 16:15	34.86866898	86436.7	86400						0.852928	109.6914	4.697671				
27	25	6/30/2022 16:49	35.89172454	86434.2	86400						1.715266	88.65741	4.48478				
28	26	7/5/2022 18:17	40.95304398	86418.8	86400						2.853669						
29											3.914236	59.93765	4.093305				
30											4.963646	45.74933	3.823177				
31											5.918623	30.16204	3.406584				
32											6.971887	27.31481	3.307429				
33											8.615266	16.99074	2.832669				
34											9.808437	13.19444	2.579796				
35											12.86723	5.409722	1.688198				
36											13.91772	4.251288	1.447222				
37											14.9169	3.333027	1.203881				
38											15.84829						
39											16.89909						
40											18.65796						
41											19.87214						
42											20.89899						
43											22.91881	0.430208	-0.84349				
44											26.05416	0.190278	-1.65927				
45																	
46																	
47																	
48																	
49																	
50																	
51																	
52																	
53																	
54																	
55																	
56																	
57																	
58																	

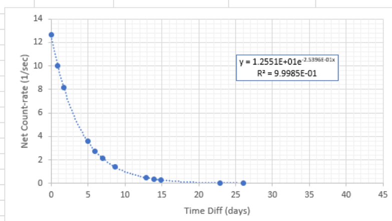

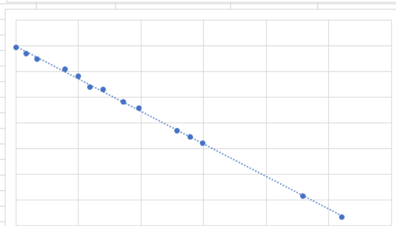

Gamma ray energy line 42 keV

	A	B	C	D	E	F	G	H	I	J	K	L	M	N	O	P	Q
1					Energy (keV) select	142											
2	Count	Count Start Date/Time	Time Diff. (days)	Realtime (sec)	Livetime (sec)	Net Peak Area	Net Count-rate (1/sec)	BAD		Log-Linear Fit							
3	1	5/25/2022 19:25	0	72870.9	62850.9	370900000	5901.267921			8.682922509			0	8.682923		-2.5209E-01	8.6552E+00
4	2	5/26/2022 15:53	0.852928241	72838.1	64800	302700000	4671.296296			8.449191892			0.852928	8.449192		2.8048E-04	5.9763E-03
5	3	5/27/2022 12:34	1.715266204	71216.6	64800	243800000	3762.345679			8.232797893			1.715266	8.232798		9.9998E-01	1.6380E-02
6	4	5/28/2022 15:54	2.853668981	91600.8	85480.5	234100000		2738.636					3.914236	7.648181		8.0783E+05	1.8000E+01
7	5	5/29/2022 17:21	3.914236111	90627	85939.3	180200000	2096.828808			7.648181391			4.963646	7.394688			
8	6	5/30/2022 18:32	4.963645833	82500.2	79148.7	128800000	1627.316684			7.394687731			5.918623	7.142864		Half-life (hrs)	65.9899
9	7	5/31/2022 17:27	5.918622685	89247.6	86400	109300000	1265.046296			7.142863998			6.971887	6.878393		`+/-	0.0733
10	8	6/1/2022 18:44	6.971886574	88584	86400	83900000	971.0648148			6.878393217			8.615266	6.46461			
11	9	6/3/2022 10:10	8.615266204	87840.1	86400	55470000	642.0138889			6.464609937			9.808437	6.16234			
12	10	6/4/2022 14:49	9.8084375	87463	86400	41000000	474.537037			6.16233967			12.86723	5.417129			
13	11	6/7/2022 16:13	12.8672338	86930.5	86400	19460000	225.2314815			5.41712868			13.91772	5.173659			
14	12	6/8/2022 17:26	13.91771991	62379.4	62075.3	10960000	176.5597589			5.173659396			14.9169	4.925787			
15	13	6/9/2022 17:25	14.91689815	65471.1	65226	8988000	137.7978107			4.925787471			22.91881	2.88055			
16	14	6/10/2022 15:46	15.84828704	86639.7	86400	699400		8.094907					26.05416	2.091235			
17	15	6/11/2022 16:59	16.89908565	86590.7	86400	#REF!		#REF!					27.82044	1.644242			
18	16	6/13/2022 11:12	18.65796296	14087.3	14060.9	804400		57.20829					29.90413	1.118475			
19	17	6/14/2022 16:20	19.8721412	86518.9	86400	#REF!							33.87206	0.113904			
20	18	6/15/2022 16:59	20.89899306	86499.8	86400	#REF!							34.86867	-0.14083			
21	19	6/17/2022 17:28	22.91880787	86469.1	86400	1540000	17.82407407			2.88055002			35.89172	-0.39923			
22	20	6/20/2022 20:42	26.05415509	86451.1	86400	699400	8.094907407			2.091235149			40.95304	-1.66844			
23	21	6/22/2022 15:06	27.82043981	86447.2	86400	447300	5.177083333			1.644241835							
24	22	6/24/2022 17:06	29.90413194	86440.8	86400	264400	3.060185185			1.118475432							
25	23	6/28/2022 16:20	33.87206019	85129.2	85093.9	95360	1.120644371			0.113903851							
26	24	6/29/2022 16:15	34.86866898	86436.7	86400	75050	0.868634259			-0.140833118							
27	25	6/30/2022 16:49	35.89172454	86434.2	86400	57960	0.670833333			-0.399234558							
28	26	7/5/2022 18:17	40.95304398	86418.8	86400	16290	0.188541667			-1.668436253							

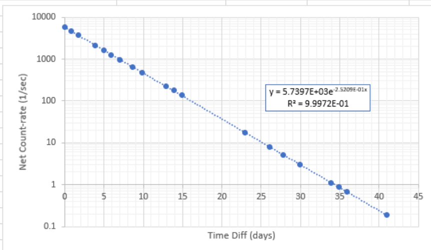

Gamma ray energy line 142 keV

	A	B	C	D	E	F	G	H	I	J	K	L	M	N	O	P	Q
1				`	Energy (keV) select	160											
2	Count	Count Start Date/Tim	Time Diff. (days)	Realtime (sec)	Livetime (sec)	Net Peak Area	Net Count-rate (1/sec)	BAD		Log-Linear Fit							
3	1	5/25/2022 19:25	0	72870.9	62850.9	996900	15.86134805			2.763885209			0	2.763885		-2.5367E-01	#########
4	2	5/26/2022 15:53	0.852928241	72838.1	64800	805100	12.42438272			2.51966089			0.852928	2.519661		1.5306E-03	1.6213E-02
5	3	5/27/2022 12:34	1.715266204	71216.6	64800	638100	9.847222222			2.287189408			1.715266	2.287189		9.9967E-01	3.4732E-02
6	4	5/28/2022 15:54	2.853668981	91600.8	85480.5	602300		7.046051					3.914236	1.681057		2.7467E+04	#########
7	5	5/29/2022 17:21	3.914236111	90627	85939.3	461600	5.371232952			1.681057482			4.963646	1.428067			
8	6	5/30/2022 18:32	4.963645833	82500.2	79148.7	330100	4.170630724			1.428067277			5.918623	1.160688		Half-life (hrs)	65.5805
9	7	5/31/2022 17:27	5.918622685	89247.6	86400	275800	3.19212963			1.16068829			6.971887	0.896655		`+/-	0.3933
10	8	6/1/2022 18:44	6.971886574	88584	86400	211800	2.451388889			0.896654757			12.86723	-0.54537			
11	9	6/3/2022 10:10	8.615266204	87840.1	86400	137300		1.58912					13.91772	-0.8008			
12	10	6/4/2022 14:49	9.8084375	87463	86400	101000		1.168981					14.9169	-1.05066			
13	11	6/7/2022 16:13	12.8672338	86930.5	86400	50080	0.57962963			-0.545365949			22.91881	-3.10289			
14	12	6/8/2022 17:26	13.91771991	62379.4	62075.3	27870	0.448970847			-0.800797323							
15	13	6/9/2022 17:25	14.91689815	65471.1	65226	22810	0.349707172			-1.050659126							
16	14	6/10/2022	15.84828704	86639.7	86400	1445											
17	15	6/11/2022 16:59	16.89908565	86590.7	86400												
18	16	6/13/2022 11:12	18.65796296	14087.3	14060.9	2293		0.163076									
19	17	6/14/2022 16:20	19.8721412	86518.9	86400												
20	18	6/15/2022 16:59	20.89899306	86499.8	86400												
21	19	6/17/2022 17:28	22.91880787	86469.1	86400	3881		0.044919		-3.102894823							
22	20	6/20/2022 20:42	26.05415509	86451.1	86400	1445		0.016725									
23	21	6/22/2022 15:06	27.82043981	86447.2	86400												
24	22	6/24/2022 17:06	29.90413194	86440.8	86400												
25	23	6/28/2022 16:20	33.87206019	85129.2	85093.9												
26	24	6/29/2022 16:15	34.86866898	86436.7	86400			0	15.86135	2.763885209							
27	25	6/30/2022 16:49	35.89172454	86434.2	86400			0.852928	12.42438	2.51966089							
28	26	7/5/2022 18:17	40.95304398	86418.8	86400			1.715266	9.847222	2.287189408							
29								2.853669									
30								3.914236	5.371233	1.681057482							
31								4.963646	4.170631	1.428067277							
32								5.918623	3.19213	1.16068829							
33								6.971887	2.451389	0.896654757							
34								8.615266	1.58912	0.463180637							
35								9.808437	1.168981	0.156132841							
36								12.86723	0.57963	-0.545365949							
37								13.91772	0.448971	-0.800797323							
38								14.9169	0.349707	-1.050659126							
39								15.84829									
40								16.89909									
41								18.65796	0.163076		-1.81354						
42								19.87214									
43								20.89899									
44								22.91881	0.044919	-3.102894823							
45								26.05416	0.016725		-4.09088						

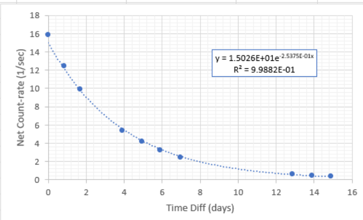

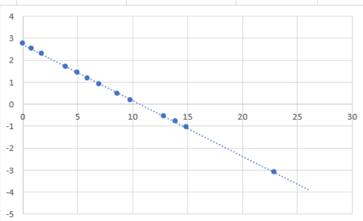

Gamma ray energy line 160 keV

	A	B	C	D	E	F	G	H	J	M	N	P	Q
1					Energy (keV) select	182							
2	Count	Count Start Date/Tim	Time Diff. (days)	Realtime (sec)	Livetime (sec)	Net Peak Area	Net Count-rate (1/sec)	BAD	Log-Linear Fit				
3	1	5/25/2022 19:25	0	72870.9	62850.9	13340000	212.2483528		5.357757065	0	5.357757	-2.5309E-01	#########
4	2	5/26/2022 15:53	0.852928241	72838.1	64800	11190000	172.6851852		5.151470198	0.852928	5.15147	5.4973E-04	1.1870E-02
5	3	5/27/2022 12:34	1.715266204	71216.6	64800	9009000	139.0277778		4.934673753	1.715266	4.934674	9.9992E-01	3.2085E-02
6	4	5/28/2022 15:54	2.853668981	91600.8	85480.5	8644000		101.1225		3.914236	4.348731	2.1196E+05	#########
7	5	5/29/2022 17:21	3.914236111	90627	85939.3	6650000	77.38019742		4.348730901	4.963646	4.088236		
8	6	5/30/2022 18:32	4.963645833	82500.2	79148.7	4720000	59.63458654		4.088235717	5.918623	3.843774	Half-life (hrs)	65.7294
9	7	5/31/2022 17:27	5.918622685	89247.6	86400	4035000	46.70138889		3.843773905	6.971887	3.58017	`+/-	0.1425
10	8	6/1/2022 18:44	6.971886574	88584	86400	3100000	35.87962963		3.580169715	8.615266	3.164654		
11	9	6/3/2022 10:10	8.615266204	87840.1	86400	2046000	23.68055556		3.164654271	9.808437	2.867478		
12	10	6/4/2022 14:49	9.8084375	87463	86400	1520000	17.59259259		2.867477938	12.86723	2.10388		
13	11	6/7/2022 16:13	12.8672338	86930.5	86400	708300	8.197916667		2.103880057	13.91772	1.861114		
14	12	6/8/2022 17:26	13.91771991	62379.4	62075.3	399200	6.430899247		1.86111438	22.91881	-0.42157		
15	13	6/9/2022 17:25	14.91689815	65471.1	65226	328400	5.034802073		1.616374215	26.05416	-1.22266		
16	14	6/10/2022 15:46	15.84828704	86639.7	86400	25440		0.294444		27.82044	-1.67336		
17	15	6/11/2022 16:59	16.89908565	86590.7	86400	#REF!				29.90413	-2.21552		
18	16	6/13/2022 11:12	18.65796296	14087.3	14060.9	29360		2.08806		33.87206	-3.17963		
19	17	6/14/2022 16:20	19.8721412	86518.9	86400	#REF!				34.86867	-3.44339		
20	18	6/15/2022 16:59	20.89899306	86499.8	86400	#REF!				35.89172	-3.68564		
21	19	6/17/2022 17:28	22.91880787	86469.1	86400	56680	0.656018519		-0.421566261	40.95304	-5.11311		
22	20	6/20/2022 20:42	26.05415509	86451.1	86400	25440	0.294444444		-1.222664937				
23	21	6/22/2022 15:06	27.82043981	86447.2	86400	16210	0.187615741		-1.67335934				
24	22	6/24/2022 17:06	29.90413194	86440.8	86400	9426	0.109097222		-2.215515847				
25	23	6/28/2022 16:20	33.87206019	85129.2	85093.9	3540	0.041601102		-3.179628625				
26	24	6/29/2022 16:15	34.86866898	86436.7	86400	2761	0.031956019		-3.443394743				
27	25	6/30/2022 16:49	35.89172454	86434.2	86400	2167	0.025081019		-3.685643953				
28	26	7/5/2022 18:17	40.95304398	86418.8	86400	519.9	0.006017361		-5.113106469				

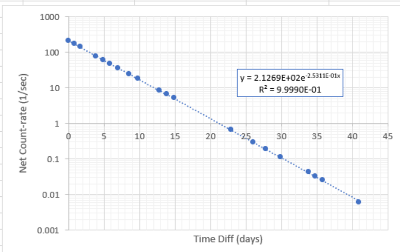

Gamma ray energy line 182 keV

	A	B	C	D	E	F	G	H	J	M	N	P	Q
1					Energy (keV) select	367							
2	Count	Count Start Date/Time	Time Diff. (days)	Realtime (sec)	Livetime (sec)	Net Peak Are:	Net Count-rate (1/sec)	BAD	Log-Linear Fit				
3	1	5/25/2022 19:25	0	72870.9	62850.9	1860000	29.5938483		3.387566512	0	3.38757	-2.5072E-01	#########
4	2	5/26/2022 15:53	0.852928241	72838.1	64800	1629000	25.13888889		3.224416005	0.85293	3.22442	1.0410E-03	#########
5	3	5/27/2022 12:34	1.715266204	71216.6	64800	1307000		20.1698	3.00418411	1.71527	3.00418	9.9974E-01	#########
6	4	5/28/2022 15:54	2.853668981	91600.8	85480.5	1258000		14.7168		3.91424	2.42097	5.8009E+04	#########
7	5	5/29/2022 17:21	3.914236111	90627	85939.3	967400	11.2567824		2.420970827	4.96365	2.16565		
8	6	5/30/2022 18:32	4.963645833	82500.2	79148.7	690200	8.720294837		2.165653049	5.91862	1.91978	Half-life (hrs)	66.3522
9	7	5/31/2022 17:27	5.918622685	89247.6	86400	589200	6.819444444		1.919778009	6.97189	1.65226	`+/-	0.2744
10	8	6/1/2022 18:44	6.971886574	88584	86400	450900	5.21875		1.65225791	8.61527	1.23205		
11	9	6/3/2022 10:10	8.615266204	87840.1	86400	296200	3.428240741		1.232047226	9.80844	0.93918		
12	10	6/4/2022 14:49	9.8084375	87463	86400	221000	2.55787037		0.939175026	12.8672	0.18348		
13	11	6/7/2022 16:13	12.8672338	86930.5	86400	103800	1.201388889		0.183478295	13.9177	-0.05523		
14	12	6/8/2022 17:26	13.91771991	62379.4	62075.3	58740	0.946270095		-0.055227238	14.9169	-0.31021		
15	13	6/9/2022 17:25	14.91689815	65471.1	65226	47830	0.733296538		-0.310205105	18.658	-1.155		
16	14	6/10/2022	15.84828704	86639.7	86400	3747		0.04337		22.9188	-2.30827		
17	15	6/11/2022 16:59	16.89908565	86590.7	86400					26.0542	-3.13803		
18	16	6/13/2022 11:12	18.65796296	14087.3	14060.9	4430	0.315058069		-1.154998312	27.8204	-3.52722		
19	17	6/14/2022 16:20	19.8721412	86518.9	86400					29.9041	-4.16781		
20	18	6/15/2022 16:59	20.89899306	86499.8	86400								
21	19	6/17/2022 17:28	22.91880787	86469.1	86400	8591	0.09943287		-2.308272532				
22	20	6/20/2022 20:42	26.05415509	86451.1	86400	3747	0.043368056		-3.138032156				
23	21	6/22/2022 15:06	27.82043981	86447.2	86400	2539	0.029386574		-3.527217373				
24	22	6/24/2022 17:06	29.90413194	86440.8	86400	1338	0.015486111		-4.167811714				
25	23	6/28/2022 16:20	33.87206019	85129.2	85093.9								
26	24	6/29/2022 16:15	34.86866898	86436.7	86400								
27	25	6/30/2022 16:49	35.89172454	86434.2	86400								
28	26	7/5/2022 18:17	40.95304398	86418.8	86400								

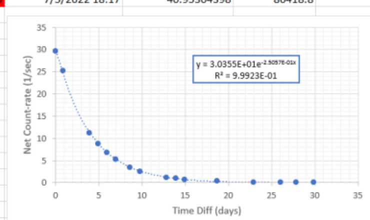

Gamma ray energy line 367 keV

	A	B	C	D	E	F	G	H	J	M	N	P	Q
1					Energy (keV) select	528							
2	Count	Count Start Date/Time	Time Diff. (days)	Realtime (sec)	Livetime (sec)	Net Peak Area	Net Count-rate (1/sec)	BAD	Log-Linear Fit				
3	1	5/25/2022 19:25	0	72870.9	62850.9	1860000	29.5938483		3.387566512	0	3.38757	-2.5077E-01	#########
4	2	5/26/2022 15:53	0.852928241	72838.1	64800	1629000	25.13888889		3.224416005	0.85293	3.22442	1.2645E-03	#########
5	3	5/27/2022 12:34	1.715266204	71216.6	64800	1307000	20.16975309		3.00418411	1.71527	3.00418	9.9977E-01	#########
6	4	5/28/2022 15:54	2.853668981	91600.8	85480.5	1258000		14.7168		3.91424	2.42097	3.9331E+04	#########
7	5	5/29/2022 17:21	3.914236111	90627	85939.3	967400	11.2567824		2.420970827	4.96365	2.16565		
8	6	5/30/2022 18:32	4.963645833	82500.2	79148.7	690200	8.720294837		2.165653049	5.91862	1.91978	Half-life (hrs)	66.3381
9	7	5/31/2022 17:27	5.918622685	89247.6	86400	589200	6.819444444		1.919778009	6.97189	1.65226	`+/-	0.3328
10	8	6/1/2022 18:44	6.971886574	88584	86400	450900	5.21875		1.65225791	8.61527	1.23205		
11	9	6/3/2022 10:10	8.615266204	87840.1	86400	296200	3.428240741		1.232047226	9.80844	0.93918		
12	10	6/4/2022 14:49	9.8084375	87463	86400	221000	2.55787037		0.939175026	12.8672	0.18348		
13	11	6/7/2022 16:13	12.8672338	86930.5	86400	103800	1.201388889		0.183478295	13.9177	-0.05523		
14	12	6/8/2022 17:26	13.91771991	62379.4	62075.3	58740	0.946270095		-0.05522724				
15	13	6/9/2022 17:25	14.91689815	65471.1	65226	47830							
16	14	6/10/2022	15.84828704	86639.7	86400	1502							
17	15	6/11/2022 16:59	16.89908565	86590.7	86400								
18	16	6/13/2022 11:12	18.65796296	14087.3	14060.9	4430							
19	17	6/14/2022 16:20	19.8721412	86518.9	86400								
20	18	6/15/2022 16:59	20.89899306	86499.8	86400								
21	19	6/17/2022 17:28	22.91880787	86469.1	86400	8591							
22	20	6/20/2022 20:42	26.05415509	86451.1	86400	1502							
23	21	6/22/2022 15:06	27.82043981	86447.2	86400								
24	22	6/24/2022 17:06	29.90413194	86440.8	86400								
25	23	6/28/2022 16:20	33.87206019	85129.2	85093.9								
26	24	6/29/2022 16:15	34.86866898	86436.7	86400								
27	25	6/30/2022 16:49	35.89172454	86434.2	86400								
28	26	7/5/2022 18:17	40.95304398	86418.8	86400								

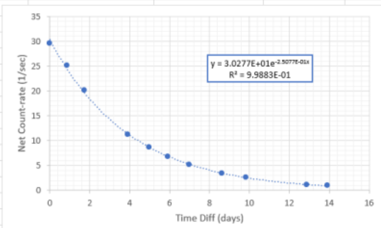

Gamma ray energy line 528 keV

	A	B	C	D	E	F	G	H	J	M	N	P	Q
1					Energy (keV) select	741							
2	Count	Count Start Date/Tim	Time Diff. (days)	Realtime (sec)	Livetime (sec)	Net Peak Area	Net Count-rate (1/sec	BAD	Log-Linear Fit				
3	1	5/25/2022 19:25	0	72870.9	62850.9	3250000	51.70968117		3.945645021	0	3.945645	-2.5374E-01	#########
4	2	5/26/2022 15:53	0.852928241	72838.1	64800	2834000	43.7345679		3.778138817	0.852928	3.778139	7.2328E-04	1.3880E-02
5	3	5/27/2022 12:34	1.715266204	71216.6	64800	2348000	36.2345679		3.590013578	1.715266	3.590014	9.9987E-01	3.7161E-02
6	4	5/28/2022 15:54	2.853668981	91600.8	85480.5	628600		7.353724		3.914236	3.007999	1.2308E+05	#########
7	5	5/29/2022 17:21	3.914236111	90627	85939.3	1740000	20.24684865		3.007999159	4.963646	2.75315		
8	6	5/30/2022 18:32	4.963645833	82500.2	79148.7	1242000	15.69198231		2.753149901	5.918623	2.50136	Half-life (hrs)	65.5608
9	7	5/31/2022 17:27	5.918622685	89247.6	86400	1054000	12.19907407		2.501360053	6.971887	2.235822	`+/-	0.1863
10	8	6/1/2022 18:44	6.971886574	88584	86400	808200	9.354166667		2.235821877	8.615266	1.823466		
11	9	6/3/2022 10:10	8.615266204	87840.1	86400	535100	6.193287037		1.82346597	9.808437	1.522427		
12	10	6/4/2022 14:49	9.8084375	87463	86400	396000	4.583333333		1.522426535	12.86723	0.752136		
13	11	6/7/2022 16:13	12.8672338	86930.5	86400	183300	2.121527778		0.752136479	13.91772	0.517964		
14	12	6/8/2022 17:26	13.91771991	62379.4	62075.3	104200	1.678606467		0.517963965	14.9169	0.260785		
15	13	6/9/2022 17:25	14.91689815	65471.1	65226	84660	1.297948671		0.260785073	22.91881	-1.7725		
16	14	6/10/2022 15:46	15.84828704	86639.7	86400	6558		0.075903		26.05416	-2.5783		
17	15	6/11/2022 16:59	16.89908565	86590.7	86400					29.90413	-3.58394		
18	16	6/13/2022 11:12	18.65796296	14087.3	14060.9	4430		0.315058		33.87206	-4.63601		
19	17	6/14/2022 16:20	19.8721412	86518.9	86400					34.86867	-4.77878		
20	18	6/15/2022 16:59	20.89899306	86499.8	86400					35.89172	-5.1793		
21	19	6/17/2022 17:28	22.91880787	86469.1	86400	14680	0.169907407		-1.772501653				
22	20	6/20/2022 20:42	26.05415509	86451.1	86400	6558	0.075902778		-2.578301997				
23	21	6/22/2022 15:06	27.82043981	86447.2	86400								
24	22	6/24/2022 17:06	29.90413194	86440.8	86400	2399	0.027766204		-3.583935692				
25	23	6/28/2022 16:20	33.87206019	85129.2	85093.9	825.1	0.009696347		-4.636006041				
26	24	6/29/2022 16:15	34.86866898	86436.7	86400	726.3	0.00840625		-4.778779802				
27	25	6/30/2022 16:49	35.89172454	86434.2	86400	486.6	0.005631944		-5.179300524				
28	26	7/5/2022 18:17	40.95304398	86418.8	86400								

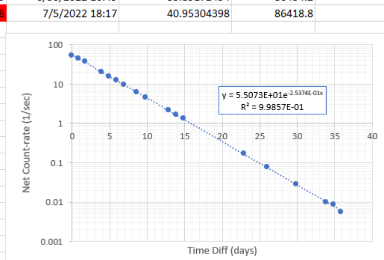

Gamma ray energy line 741 keV

	A	B	C	D	E	F	G	H	J	M	N	P	Q
1				`	Energy (keV) select	778.7							
2	Count	Count Start Date/Tim	Time Diff. (days)	Realtime (sec)	Livetime (sec)	Net Peak Are	Net Count-rate (1/sec	BAD	Log-Linear Fit				
3	1	5/25/2022 19:25	0	72870.9	62850.9	3367000	53.57122969		3.981012164	0	3.981012	-2.5256E-01	#########
4	2	5/26/2022 15:53	0.852928241	72838.1	64800	2769000	42.73148148		3.75493592	0.852928	3.754936	7.0763E-04	1.3968E-02
5	3	5/27/2022 12:34	1.715266204	71216.6	64800	2303000	35.54012346		3.570662296	1.715266	3.570662	9.9987E-01	3.7433E-02
6	4	5/28/2022 15:54	2.853668981	91600.8	85480.5	1592000		18.62413		3.914236	2.983565	1.2738E+05	#########
7	5	5/29/2022 17:21	3.914236111	90627	85939.3	1698000	19.75813161		2.983565134	4.963646	2.728699		
8	6	5/30/2022 18:32	4.963645833	82500.2	79148.7	1212000	15.31294892		2.728698805	5.918623	2.479297	Half-life (hrs)	65.8688
9	7	5/31/2022 17:27	5.918622685	89247.6	86400	1031000	11.93287037		2.479296808	6.971887	2.214942	`+/-	0.1840
10	8	6/1/2022 18:44	6.971886574	88584	86400	791500	9.16087963		2.214942204	8.615266	1.798488		
11	9	6/3/2022 10:10	8.615266204	87840.1	86400	521900	6.040509259		1.798488323	9.808437	1.499437		
12	10	6/4/2022 14:49	9.8084375	87463	86400	387000	4.479166667		1.499437017	12.86723	0.634149		
13	11	6/7/2022 16:13	12.8672338	86930.5	86400	162900	1.885416667		0.63414884	13.91772	0.512189		
14	12	6/8/2022 17:26	13.91771991	62379.4	62075.3	103600	1.668940786		0.512189166	14.9169	0.256049		
15	13	6/9/2022 17:25	14.91689815	65471.1	65226	84260	1.291816147		0.256049094	22.91881	-1.78002		
16	14	6/10/2022	15.84828704	86639.7	86400	6623		0.076655		26.05416	-2.56844		
17	15	6/11/2022 16:59	16.89908565	86590.7	86400					27.82044	-2.99365	.	
18	16	6/13/2022 11:12	18.65796296	14087.3	14060.9	7616		0.541644		29.90413	-3.58937		
19	17	6/14/2022 16:20	19.8721412	86518.9	86400					33.87206	-4.55056		
20	18	6/15/2022 16:59	20.89899306	86499.8	86400					34.86867	-4.88931		
21	19	6/17/2022 17:28	22.91880787	86469.1	86400	14570	0.168634259		-1.78002306	35.89172	-5.10106		
22	20	6/20/2022 20:42	26.05415509	86451.1	86400	6623	0.076655093		-2.56843924				
23	21	6/22/2022 15:06	27.82043981	86447.2	86400	4329	0.050104167		-2.99365111				
24	22	6/24/2022 17:06	29.90413194	86440.8	86400	2386	0.027615741		-3.58936935				
25	23	6/28/2022 16:20	33.87206019	85129.2	85093.9	898.7	0.010561274		-4.55056136				
26	24	6/29/2022 16:15	34.86866898	86436.7	86400	650.3	0.00752662		-4.88930916				
27	25	6/30/2022 16:49	35.89172454	86434.2	86400	526.2	0.006090278		-5.10106159				
28	26	7/5/2022 18:17	40.95304398	86418.8	86400								

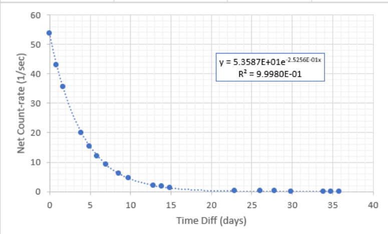

Gamma ray energy line 778.7 keV

	A	B	C	D	E	F	G	H	J	M	N	P	Q
1				`	Energy (keV) select	881							
2	Count	Count Start Date/Time	Time Diff. (days)	Realtime (sec)	Livetime (sec)	Net Peak Area	Net Count-rate (1/sec)	BAD	Log-Linear Fit				
3	1	5/25/2022 19:25	0	72870.9	62850.9	1547000	24.61380824		3.203307596	0	3.20331	-2.5305E-01	#########
4	2	5/26/2022 15:53	0.852928241	72838.1	64800	1257000	19.39814815		2.965177605	0.85293	2.96518	5.3314E-04	#########
5	3	5/27/2022 12:34	1.715266204	71216.6	64800	1056000	16.2962963		2.790937861	1.71527	2.79094	9.9993E-01	#########
6	4	5/28/2022 15:54	2.853668981	91600.8	85480.5	284200		3.32473		3.91424	2.20321	2.2528E+05	#########
7	5	5/29/2022 17:21	3.914236111	90627	85939.3	778100	9.054064904		2.203213818	4.96365	1.94728		
8	6	5/30/2022 18:32	4.963645833	82500.2	79148.7	554800	7.009590808		1.947279327	5.91862	1.69438	Half-life (hrs)	65.7406
9	7	5/31/2022 17:27	5.918622685	89247.6	86400	470300	5.443287037		1.694383113	6.97189	1.42989	`+/-	0.1382
10	8	6/1/2022 18:44	6.971886574	88584	86400	361000	4.178240741		1.429890283	8.61527	1.01664		
11	9	6/3/2022 10:10	8.615266204	87840.1	86400	238800	2.763888889		1.016638706	9.80844	0.71716		
12	10	6/4/2022 14:49	9.8084375	87463	86400	177000	2.048611111		0.717162057	12.8672	-0.01846		
13	11	6/7/2022 16:13	12.8672338	86930.5	86400	84820	0.981712963		-0.01845631	13.9177	-0.26426		
14	12	6/8/2022 17:26	13.91771991	62379.4	62075.3	47660	0.7677772		-0.26425569	14.9169	-0.51455		
15	13	6/9/2022 17:25	14.91689815	65471.1	65226	38990	0.597767761		-0.51455296	22.9188	-2.57056		
16	14	6/10/2022	15.84828704	86639.7	86400	2913		0.03372		26.0542	-3.3898		
17	15	6/11/2022 16:59	16.89908565	86590.7	86400					29.9041	-4.36186		
18	16	6/13/2022 11:12	18.65796296	14087.3	14060.9	7745		0.55082		33.8721	-5.38665		
19	17	6/14/2022 16:20	19.8721412	86518.9	86400					34.8687	-5.63275		
20	18	6/15/2022 16:59	20.89899306	86499.8	86400								
21	19	6/17/2022 17:28	22.91880787	86469.1	86400	6609	0.076493056		-2.57055532				
22	20	6/20/2022 20:42	26.05415509	86451.1	86400	2913	0.033715278		-3.3898042				
23	21	6/22/2022 15:06	27.82043981	86447.2	86400								
24	22	6/24/2022 17:06	29.90413194	86440.8	86400	1102	0.01275463		-4.36186097				
25	23	6/28/2022 16:20	33.87206019	85129.2	85093.9	389.5	0.004577296		-5.38664677				
26	24	6/29/2022 16:15	34.86866898	86436.7	86400	309.2	0.003578704		-5.63275464				
27	25	6/30/2022 16:49	35.89172454	86434.2	86400								
28	26	7/5/2022 18:17	40.95304398	86418.8	86400								

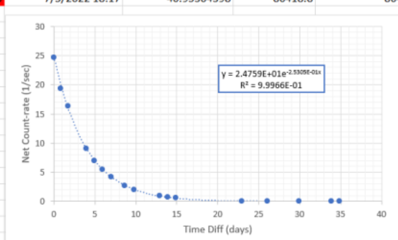

Gamma ray energy line 881 keV

	A	B	C	D	E	F	G	H	I	J	M	N	P	Q
1					**Energy (keV) select**	922								
2	**Count**	**Count Start Date/Tim**	**Time Diff. (days)**	**Realtime (sec)**	**Livetime (sec)**	**Net Peak Are**	**Net Count-rate (1/sec**	**BAD**		**Log-Linear Fit**				
3	1	5/25/2022 19:25	0	72870.9	62850.9	2366000	37.64464789			3.62819079	0	3.628191	-2.5245E-01	#########
4	2	5/26/2022 15:53	0.852928241	72838.1	64800	1905000	29.39814815			3.380931684	0.852928	3.380932	9.0727E-04	1.7909E-02
5	3	5/27/2022 12:34	1.715266204	71216.6	64800	1620000	25			3.218875825	1.715266	3.218876	9.9978E-01	4.7993E-02
6	4	5/28/2022 15:54	2.853668981	91600.8	85480.5	437200		5.114617			3.914236	2.630585	7.7424E+04	#########
7	5	5/29/2022 17:21	3.914236111	90627	85939.3	1193000	13.88189106			2.630585189	4.963646	2.380591		
8	6	5/30/2022 18:32	4.963645833	82500.2	79148.7	855700	10.8112957			2.380591486	5.918623	2.122622	Half-life (hrs)	65.8967
9	7	5/31/2022 17:27	5.918622685	89247.6	86400	721700	8.353009259			2.122621864	6.971887	1.859259	`+/-	0.2360
10	8	6/1/2022 18:44	6.971886574	88584	86400	554600	6.418981481			1.859259457	8.615266	1.445011		
11	9	6/3/2022 10:10	8.615266204	87840.1	86400	366500	4.241898148			1.445010846	9.808437	1.135724		
12	10	6/4/2022 14:49	9.8084375	87463	86400	269000	3.113425926			1.135723704	12.86723	0.416973		
13	11	6/7/2022 16:13	12.8672338	86930.5	86400	131100	1.517361111			0.416972715	13.91772	0.159368		
14	12	6/8/2022 17:26	13.91771991	62379.4	62075.3	72800	1.172769201			0.159367791	14.9169	-0.07621		
15	13	6/9/2022 17:25	14.91689815	65471.1	65226	60440	0.926624352			-0.076207025	22.91881	-2.12297		
16	14	6/10/2022	15.84828704	86639.7	86400	4722		0.054653			26.05416	-2.90676		
17	15	6/11/2022 16:59	16.89908565	86590.7	86400						27.82044	-3.36271		
18	16	6/13/2022 11:12	18.65796296	14087.3	14060.9	3487		0.247993			29.90413	-3.8835		
19	17	6/14/2022 16:20	19.8721412	86518.9	86400						33.87206	-4.97597		
20	18	6/15/2022 16:59	20.89899306	86499.8	86400						34.86867	-5.09273		
21	19	6/17/2022 17:28	22.91880787	86469.1	86400	10340	0.119675926			-2.122967807	35.89172	-5.5583		
22	20	6/20/2022 20:42	26.05415509	86451.1	86400	4722	0.054652778			-2.906755237				
23	21	6/22/2022 15:06	27.82043981	86447.2	86400	2993	0.034641204			-3.362711447				
24	22	6/24/2022 17:06	29.90413194	86440.8	86400	1778	0.020578704			-3.883498539				
25	23	6/28/2022 16:20	33.87206019	85129.2	85093.9	587.3	0.006901787			-4.975974869				
26	24	6/29/2022 16:15	34.86866898	86436.7	86400	530.6	0.006141204			-5.092734513				
27	25	6/30/2022 16:49	35.89172454	86434.2	86400	333.1	0.003855324			-5.55830021				
28	26	7/5/2022 18:17	40.95304398	86418.8	86400									
29							0	37.64465	3.628191					
30							0.852928241	29.39815	3.380932					
31							1.715266204	25	3.218876					
32							2.853668981							
33							3.914236111	13.88189	2.630585					
34							4.963645833	10.8113	2.380591					
35							5.918622685	8.353009	2.122622					
36							6.971886574	6.418981	1.859259					
37							8.615266204	4.241898	1.445011					
38							9.8084375	3.113426	1.135724					
39							12.8672338	1.517361	0.416973					
40							13.91771991	1.172769	0.159368					
41							14.91689815	0.926624	-0.07621					
42							15.84828704							
43							16.89908565							
44							18.65796296	0.247993	-1.39436					
45							19.8721412							
46							20.89899306							
47							22.91880787	0.119676	-2.12297					
48							26.05415509	0.054653	-2.90676					

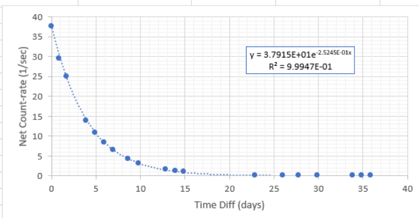

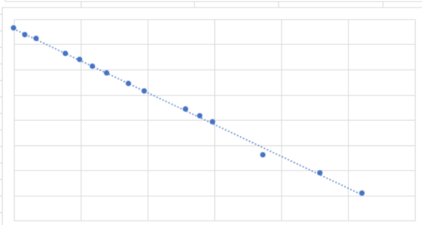

Gamma ray energy line 922 keV

	A	B	C	D	E	F	G	H	J	M	N	P	Q
1					Energy (keV) select	1005							
2	Count	Count Start Date/Tim	Time Diff. (days)	Realtime (sec)	Livetime (sec)	Net Peak Are:	Net Count-rate (1/sec	BAD	Log-Linear Fit				
3	1	5/25/2022 19:25	0	72870.9	62850.9	25870	0.411609062		-0.88768126	0	-0.88768	-2.5614E-01	-8.6801E-01
4	2	5/26/2022 15:53	0.852928241	72838.1	64800	22480	0.34691358		-1.05867958	0.85293	-1.05868	1.3730E-03	1.0611E-02
5	3	5/27/2022 12:34	1.715266204	71216.6	64800	17300	0.266975309		-1.3205991	1.71527	-1.3206	9.9974E-01	2.0238E-02
6	4	5/28/2022 15:54	2.853668981	91600.8	85480.5	4565		0.0534		3.91424	-1.88946	3.4803E+04	9.0000E+00
7	5	5/29/2022 17:21	3.914236111	90627	85939.3	12990	0.151153198		-1.8894614	4.96365	-2.10904		
8	6	5/30/2022 18:32	4.963645833	82500.2	79148.7	9605	0.121353857		-2.10904457	5.91862	-2.38355	Half-life (hrs)	64.9472
9	7	5/31/2022 17:27	5.918622685	89247.6	86400	7968	0.092222222		-2.38355416	6.97189	-2.64906	`+/-	0.3463
10	8	6/1/2022 18:44	6.971886574	88584	86400	6110	0.070717593		-2.6490609	8.61527	-3.09647		
11	9	6/3/2022 10:10	8.615266204	87840.1	86400	3906	0.045208333		-3.09647384	9.80844	-3.36038		
12	10	6/4/2022 14:49	9.8084375	87463	86400	3000	0.034722222		-3.36037539	12.8672	-4.17682		
13	11	6/7/2022 16:13	12.8672338	86930.5	86400	1326	0.015347222		-4.17682078	13.9177	-4.42959		
14	12	6/8/2022 17:26	13.91771991	62379.4	62075.3	739.9	0.011919395		-4.4295884				
15	13	6/9/2022 17:25	14.91689815	65471.1	65226	431.1		0.00661					
16	14	6/10/2022	15.84828704	86639.7	86400	586.1		0.00678					
17	15	6/11/2022 16:59	16.89908565	86590.7	86400								
18	16	6/13/2022 11:12	18.65796296	14087.3	14060.9	5335		0.37942					
19	17	6/14/2022 16:20	19.8721412	86518.9	86400								
20	18	6/15/2022 16:59	20.89899306	86499.8	86400								
21	19	6/17/2022 17:28	22.91880787	86469.1	86400	10340		0.11968					
22	20	6/20/2022 20:42	26.05415509	86451.1	86400	4722		0.05465					
23	21	6/22/2022 15:06	27.82043981	86447.2	86400								
24	22	6/24/2022 17:06	29.90413194	86440.8	86400								
25	23	6/28/2022 16:20	33.87206019	85129.2	85093.9								
26	24	6/29/2022 16:15	34.86866898	86436.7	86400								
27	25	6/30/2022 16:49	35.89172454	86434.2	86400								
28	26	7/5/2022 18:17	40.95304398	86418.8	86400								

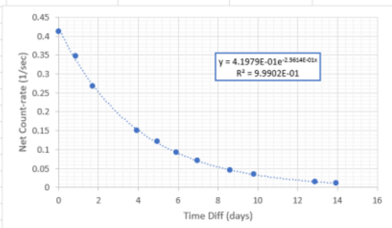

Gamma ray energy line 1005 keV

	A	B	C	D	E	F	G	H	J	M	N	P	Q
1					Energy (keV) select	1145							
2	Count	Count Start Date/Tim	Time Diff. (days)	Realtime (sec)	Livetime (sec)	Net Peak Area	Net Count-rate (1/sec)	BAD	Log-Linear Fit				
3	1	5/25/2022 19:25	0	72870.9	62850.9	16840	0.267935702		-1.317008246	0	-1.31701	-2.5321E-01	-1.3257E+00
4	2	5/26/2022 15:53	0.852928241	72838.1	64800	13980	0.215740741		-1.533677867	0.852928	-1.53368	1.8766E-03	1.3155E-02
5	3	5/27/2022 12:34	1.715266204	71216.6	64800	11480	0.177160494		-1.730699212	1.715266	-1.7307	9.9956E-01	2.4480E-02
6	4	5/28/2022 15:54	2.853668981	91600.8	85480.5	3283		0.038406		3.914236	-2.32529	1.8206E+04	8.0000E+00
7	5	5/29/2022 17:21	3.914236111	90627	85939.3	8401	0.097755043		-2.325290487	4.963646	-2.59468		
8	6	5/30/2022 18:32	4.963645833	82500.2	79148.7	5910	0.074669578		-2.59468253	5.918623	-2.82661	Half-life (hrs)	65.6975
9	7	5/31/2022 17:27	5.918622685	89247.6	86400	5116	0.059212963		-2.826614792	6.971887	-3.11273	`+/-	0.4833
10	8	6/1/2022 18:44	6.971886574	88584	86400	3843	0.044479167		-3.112734364	8.615266	-3.5395		
11	9	6/3/2022 10:10	8.615266204	87840.1	86400	2508	0.029027778		-3.539502053	9.808437	-3.82241		
12	10	6/4/2022 14:49	9.8084375	87463	86400	1890	0.021875		-3.822410847	13.91772	-4.80641		
13	11	6/7/2022 16:13	12.8672338	86930.5	86400	940.7	0.010887731						
14	12	6/8/2022 17:26	13.91771991	62379.4	62075.3	507.6	0.008177165		-4.806409707				
15	13	6/9/2022 17:25	14.91689815	65471.1	65226	353.4		0.005418					
16	14	6/10/2022 15:46	15.84828704	86639.7	86400	451.6							
17	15	6/11/2022 16:59	16.89908565	86590.7	86400			0.005227					
18	16	6/13/2022 11:12	18.65796296	14087.3	14060.9	5335							
19	17	6/14/2022 16:20	19.8721412	86518.9	86400								
20	18	6/15/2022 16:59	20.89899306	86499.8	86400								
21	19	6/17/2022 17:28	22.91880787	86469.1	86400	10340							
22	20	6/20/2022 20:42	26.05415509	86451.1	86400	4722							
23	21	6/22/2022 15:06	27.82043981	86447.2	86400								
24	22	6/24/2022 17:06	29.90413194	86440.8	86400								
25	23	6/28/2022 16:20	33.87206019	85129.2	85093.9								
26	24	6/29/2022 16:15	34.86866898	86436.7	86400								
27	25	6/30/2022 16:49	35.89172454	86434.2	86400								
28	26	7/5/2022 18:17	40.95304398	86418.8	86400								

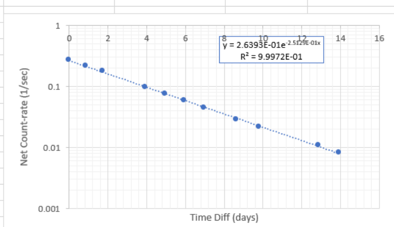

Gamma ray energy line 1145 keV

	A	B	C	D	E	F	G	H
1	**Gamma-Ray Energy Line**	**Half-Life**	**Uncertainty**					
2	41	65.5056	0.13400791		65.88767418	65.6420385	66.13330983	65.924
3	142	65.98988	0.0733391		65.88767418	65.6420385	66.13330983	65.924
4	160	65.58052	0.39333227		65.88767418	65.6420385	66.13330983	65.924
5	182	66.10041	0.25122138		65.88767418	65.6420385	66.13330983	65.924
6	367	66.48553	0.28936956		65.88767418	65.6420385	66.13330983	65.924
7	528	66.33807	0.33282215		65.88767418	65.6420385	66.13330983	65.924
8	741	65.56076	0.18634609		65.88767418	65.6420385	66.13330983	65.924
9	778.7	65.86884	0.18404133		65.88767418	65.6420385	66.13330983	65.924
10	881	65.74062	0.1382163		65.88767418	65.6420385	66.13330983	65.924
11	992	65.89666	0.23597618		65.88767418	65.6420385	66.13330983	65.924
12	1145	65.69752	0.48331993		65.88767418	65.6420385	66.13330983	65.924
13					65.88767418	65.6420385	66.13330983	65.924
14					65.88767418	65.6420385	66.13330983	65.924
15					65.88767418	65.6420385	66.13330983	65.924
16					65.88767418	65.6420385	66.13330983	65.924
17					65.88767418	65.6420385	66.13330983	65.924
18					65.88767418	65.6420385	66.13330983	65.924
19	**average**	65.88767	0.24563565					
20								
21								
22	1005	64.9472	0.34628072					
23								
24								
25								
26								
27								
28								
29								

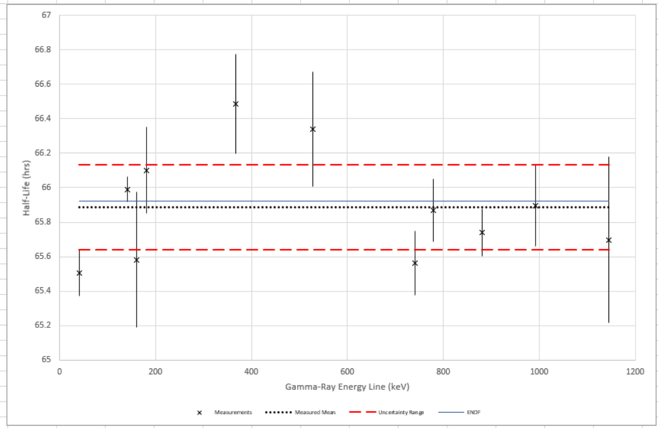

Compiled $T_{1/2}$ calculations